

MICROCOPY RESOLUTION TEST CHART
NATIONAL BUREAU OF STANDARDS-1963-A

3

NORDA-Technical Note-250 ✓

Naval Ocean Research and
Development Activity
NSTL, Mississippi 39529

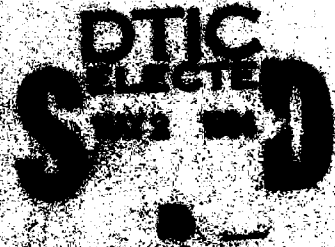


Analyzing Temperature Data from XBT Grid Surveys

AD-A140 685



DTIC FILE COPY



ABSTRACT

This report considers a set of 78 XBT casts obtained by NAVOCEANO on the second leg of its cruise to the Norwegian Sea, Spring 1981. The data were taken in a grid pattern over a rectangular segment of ocean 66.95 -- 67.40 deg N latitude and -5.60 -- -4.35 deg W longitude, in a day and a half. The survey was to measure the spatial properties of the temperature field. This report analyzes the data with that perspective, and focuses on estimating isotherm surfaces as characterizations of the temperature field.

The data from each cast are reduced to a set of depths at which the temperatures 0, 1, 2, and 3 deg C occurred. With these depths as data, two techniques are considered for estimating isotherm-depth maps: a two-dimensional Fourier series analysis, and an optimal objective analysis. Calculations of the spatial and temporal correlation of the data indicate that these analyses cannot be legitimately applied; and that a spatial characterization of this area is not possible with this data set. Mean depth and slope statistics for the isotherm depths are given.

To complete the work, a discourse on measurement error with XBTs is presented, especially as it relates to the estimation of isotherm depths.

S DTIC
ELECTE **D**
MAY 2 1984
B

Accession For	
NTIS GRA&I	<input checked="" type="checkbox"/>
DTIC TAB	<input type="checkbox"/>
Unannounced	<input type="checkbox"/>
Justification	
By	
Distribution/	
Availability Codes	
Dist	Avail and/or Special
A-1	

DTIC
ADD

ANALYZING TEMPERATURE DATA FROM XBT GRID SURVEYS

INTRODUCTION

It is sometimes desirable to obtain information on the spatial features of the oceanic temperature field. Ideally, one would sample this field at many points simultaneously to produce an instantaneous "snapshot" of what the field looked like at some point in time. But usually a researcher does not have the resources to deploy a battery of instruments over the area, and he must settle for taking measurements sequentially--moving from place to place in the field until the field is fully sampled. Of course, while this data-taking process is going on, the field itself is changing.

Gathering data synoptically can be approximated by sequential sampling if the vehicle for carrying the instrument can cover the area of concern in a time that is short compared to the time it takes the field to change. Airplanes zigzagging over limited domains and making measurements by means of dropped sensors can yield almost synoptic sampling.

For ships, the standard procedure for obtaining temperature information on the ocean is to lower by cable an instrument that measures temperature--e.g., a conductivity, temperature, and depth sensor (CTD). Although profiles from this method are exceptionally accurate, the technique cannot provide synoptic sampling because the time of making a measurement and the time of moving between sample points is too long.

A better shipborne device, at least from the point of view of obtaining quick measurements, is the expendable bathythermograph (XBT). This device can record profiles from a moving ship, and so can reduce the lag time between measurements. Only the speed of the ship limits the data-taking capability. But because ships move relatively slowly, even this technique does not closely approximate simultaneous sampling.

What, then, are the possibilities of obtaining spatial information from a ship? This report addresses that question. Using XBT grid data taken on the spring 1981 NAVOCEANO cruise to the Norwegian Sea, we present some results and some considerations in designing and carrying out further spatial studies.

THE DATA SET

On the second leg of NAVOCEANO's Spring 1981 cruise to the Norwegian Sea, an XBT survey was conducted over a rectangular area of the ocean. This area, delineated by 66.95° - 67.40° N latitude and -5.60° -- -4.35° W longitude, was uniformly sampled in a day and a half. A total of 90 T-7 XBTs were cast. Seventy-eight yielded good data. Figure 1 shows the casts by number and their respective locations. Note that an initial diagonal run preceded the constant latitude traverses.

Data from these casts (361-451) were processed by NAVOCEANO and were made available to us as temperature records in 1-meter (m) depth increments. We further processed these 78 profiles to produce our working data set. Our working set consisted of just a few numbers for each cast: the depths at which the temperature

LOCATION OF CASTS BY NUMBER

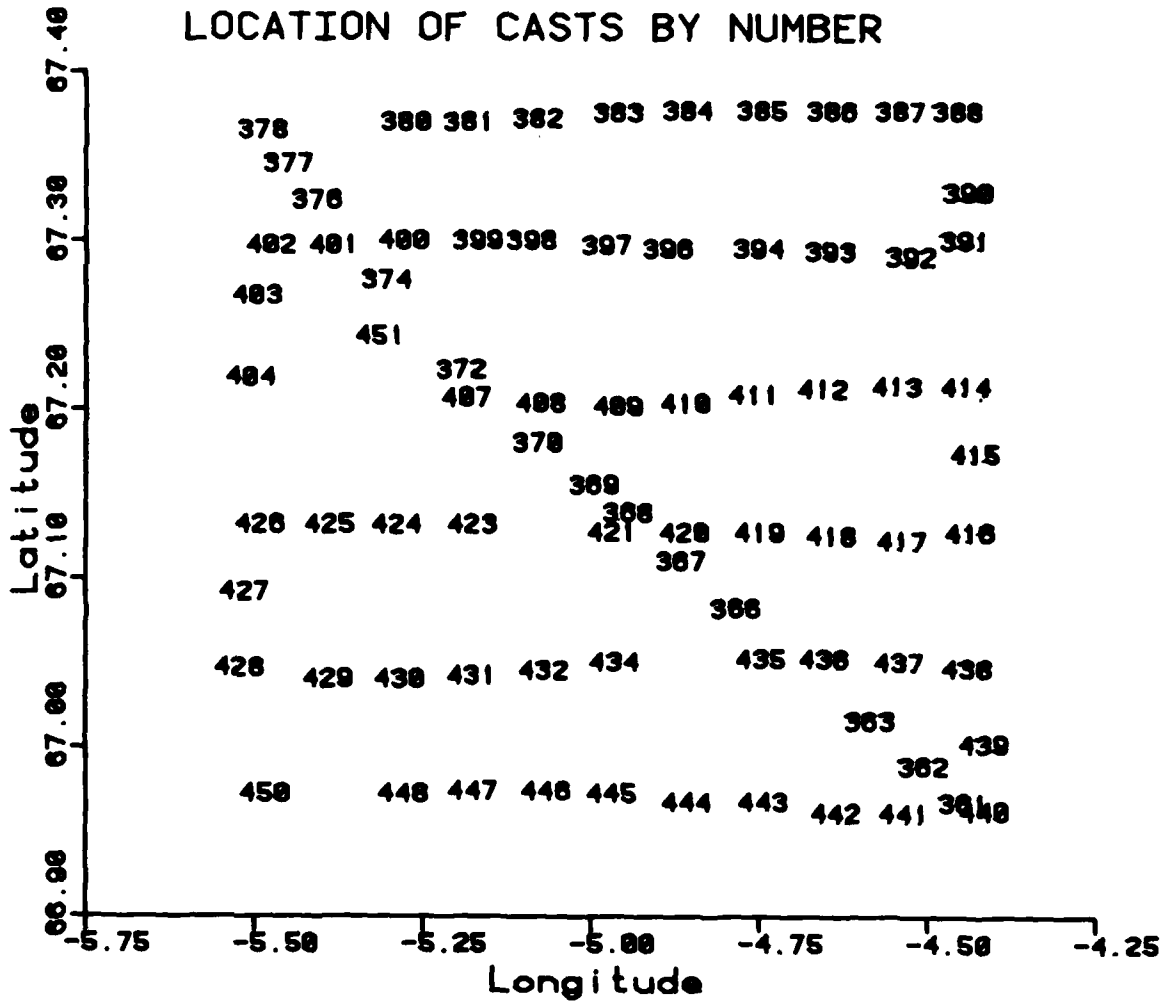


Figure 1

became an integer value (in these data, 0.0, 1.0, 2.0, and 3.0 degrees Centigrade were the only values applicable), and the local vertical temperature gradient at each of these depths.

Because of small-scale temperature inversions, an integer temperature did not always occur at just a single depth. We compensated for that by smoothing the raw profile with a five-point (5 m), cosine-weighted, butted average yielding a smoothed profile at 5-m intervals. We then chose the isotherm depth to be the first (least deep) occurrence at which an interpolated temperature was integer. Vertical temperature gradients were calculated from the smoothed profiles at that depth using adjacent smoothed values. Hence, gradients were estimated over a 5-meter depth difference.

This working set is portrayed in Figures 2(a-d) and 3(a-d) corresponding to two representations of each of the four isotherm depths. The "2" figures simply list the isotherm depths for each cast by cast location; the "3" figures give qualitative pictures of the isotherm surface contours. In "3," the contour lines are equi-spaced at 10-m depth intervals so that the density of the lines indicates slope of the surface.

QUESTIONS FOR ANALYSIS

When a researcher carries out an experiment in which he spatially samples a segment of the ocean as rapidly as possible, he is hoping that the data from that experiment will give him a picture of the spatial characteristics of that field. That was the case with the survey producing the present data set. The question becomes: How "frozen" was the field during the sampling; i.e., to what extent were the variations in the measurements due to spatial differences rather than to temporal differences? In answering that question, one can determine what sorts of spatial studies are possible from single-ship efforts.

Depending on that answer, one can then ask the related question: How closely spaced should samples be taken to resolve the significant spatial features of the field? There are, of course, features at every scale from centimeters to hundreds of kilometers. Each scale contributes some amount to the total variation in the field. In mapping out the features of a given segment of the ocean, one would like to account for an appreciable fraction of its total variation. To do so requires sampling at sufficiently small intervals, so that the features of the smallest scales that significantly contribute to the field's variation are sampled at least several times per feature. Another way of stating this requirement is to say that the distance between sample points must be somewhat smaller than the spatial scale of the field.

If the answers to the above questions can be met satisfactorily in a shipborne survey experiment, then one can ask: How best can the data be used to produce maps that characterize the field? In our case this question becomes: How can we best estimate isotherm surfaces? "Best" can carry many definitions, and so there can be no unique answer. However, we can offer several alternate schemes and elaborate on the features of each.

A final question is: How good are our estimates? In view of the fact that our measuring instruments may not provide perfectly accurate data--as is likely, using XBTs as probes--we would like to assign error bands to our estimated isotherm surfaces. Features in these surfaces may be more a manifestation of instrument error

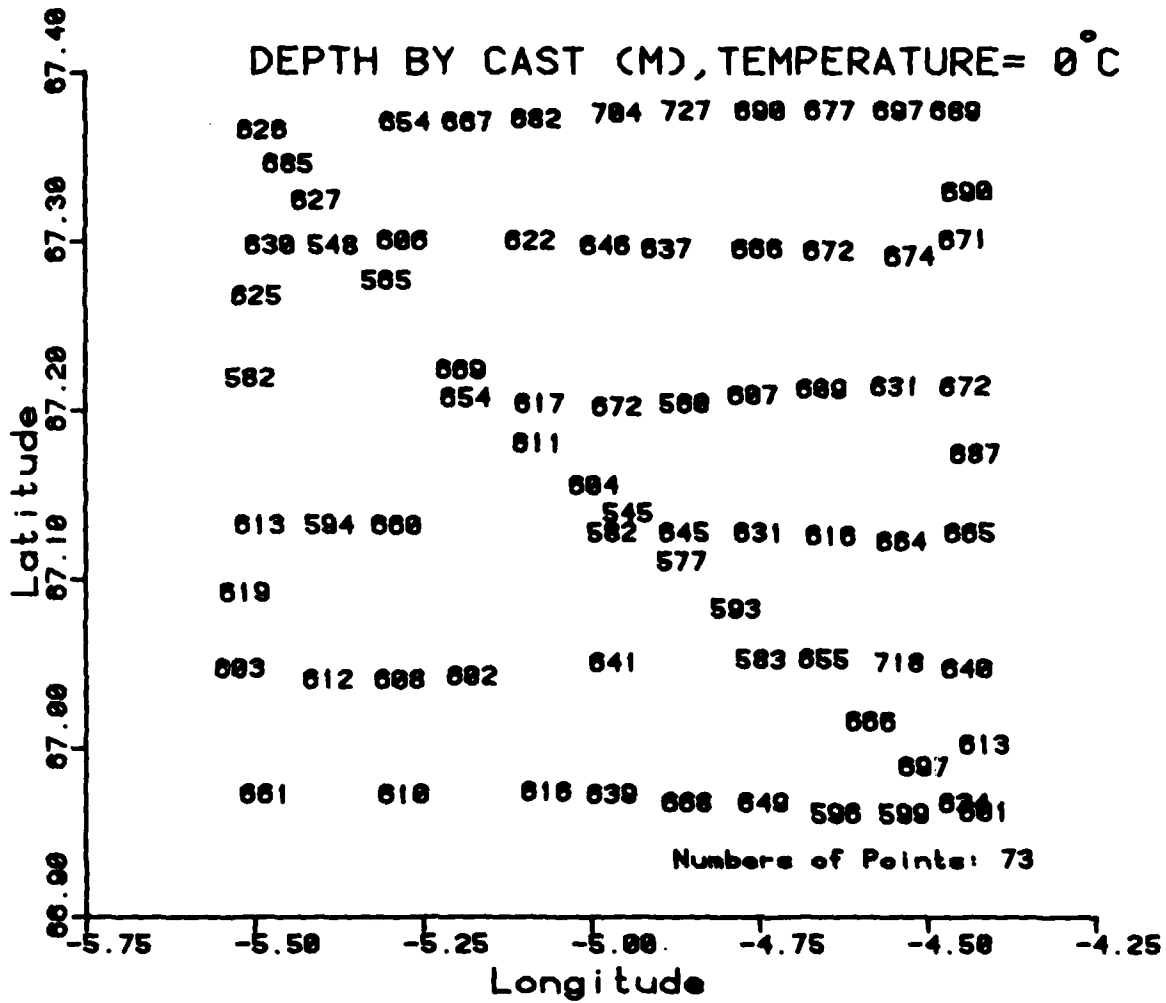


Figure 2 a)

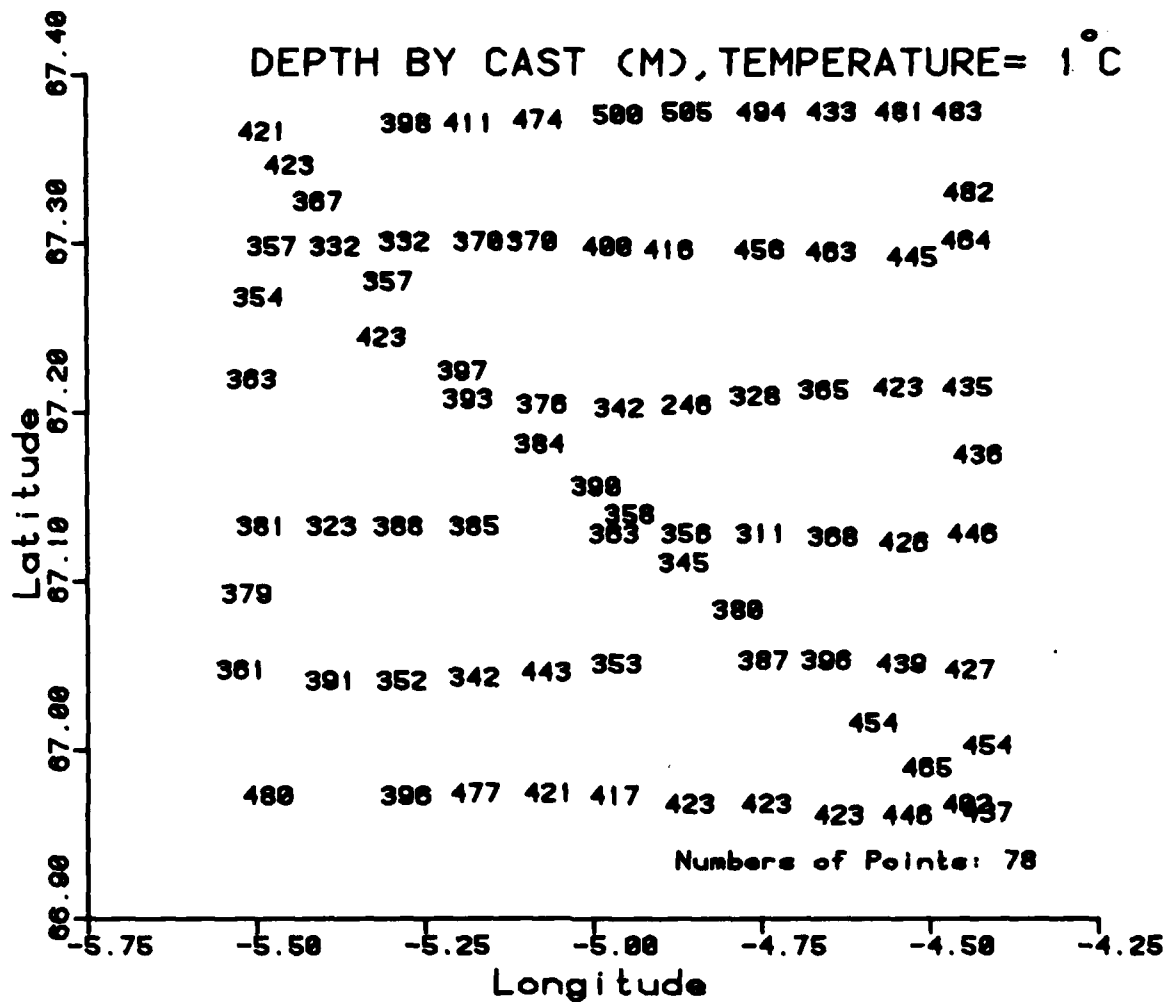


Figure 2 b)

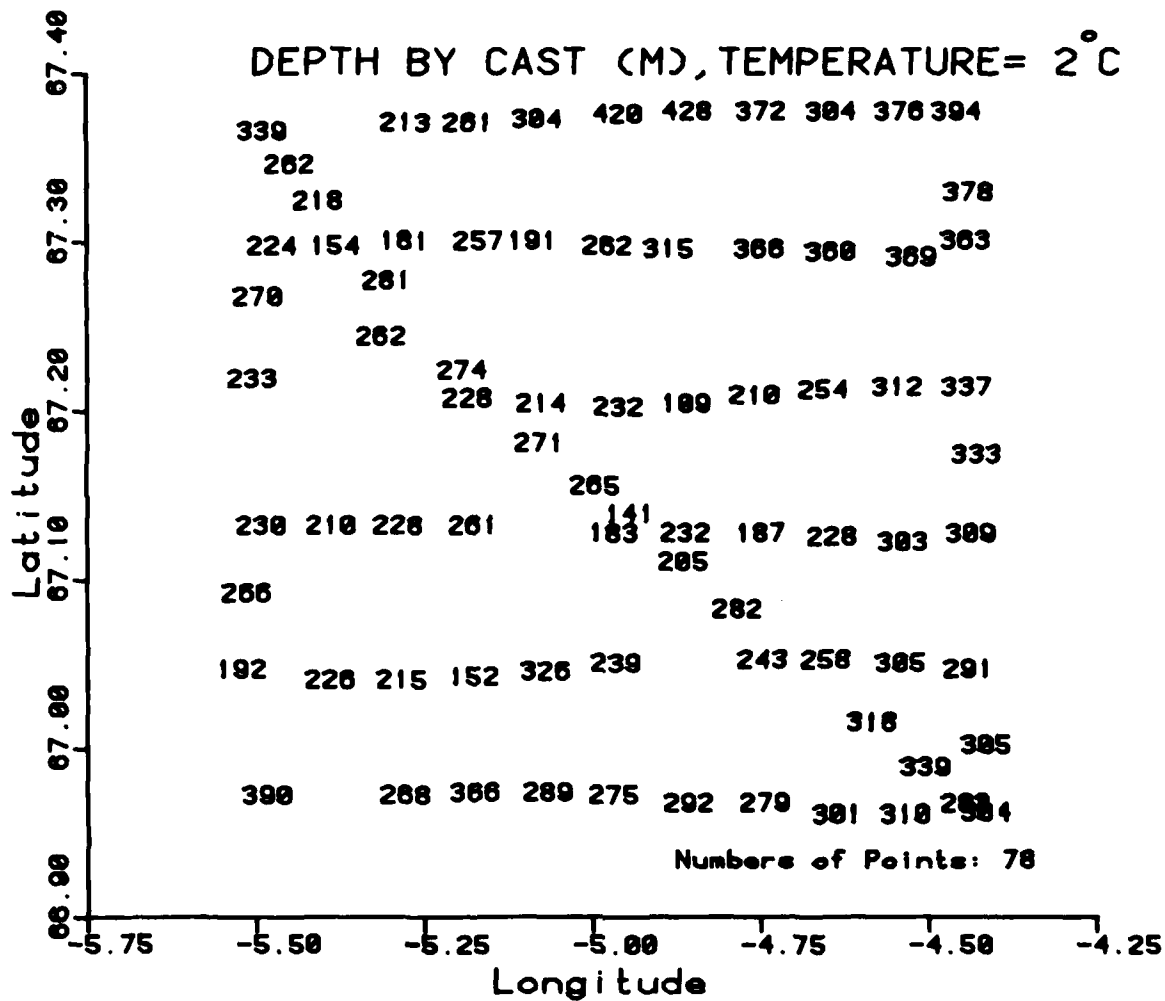


Figure 2 c)

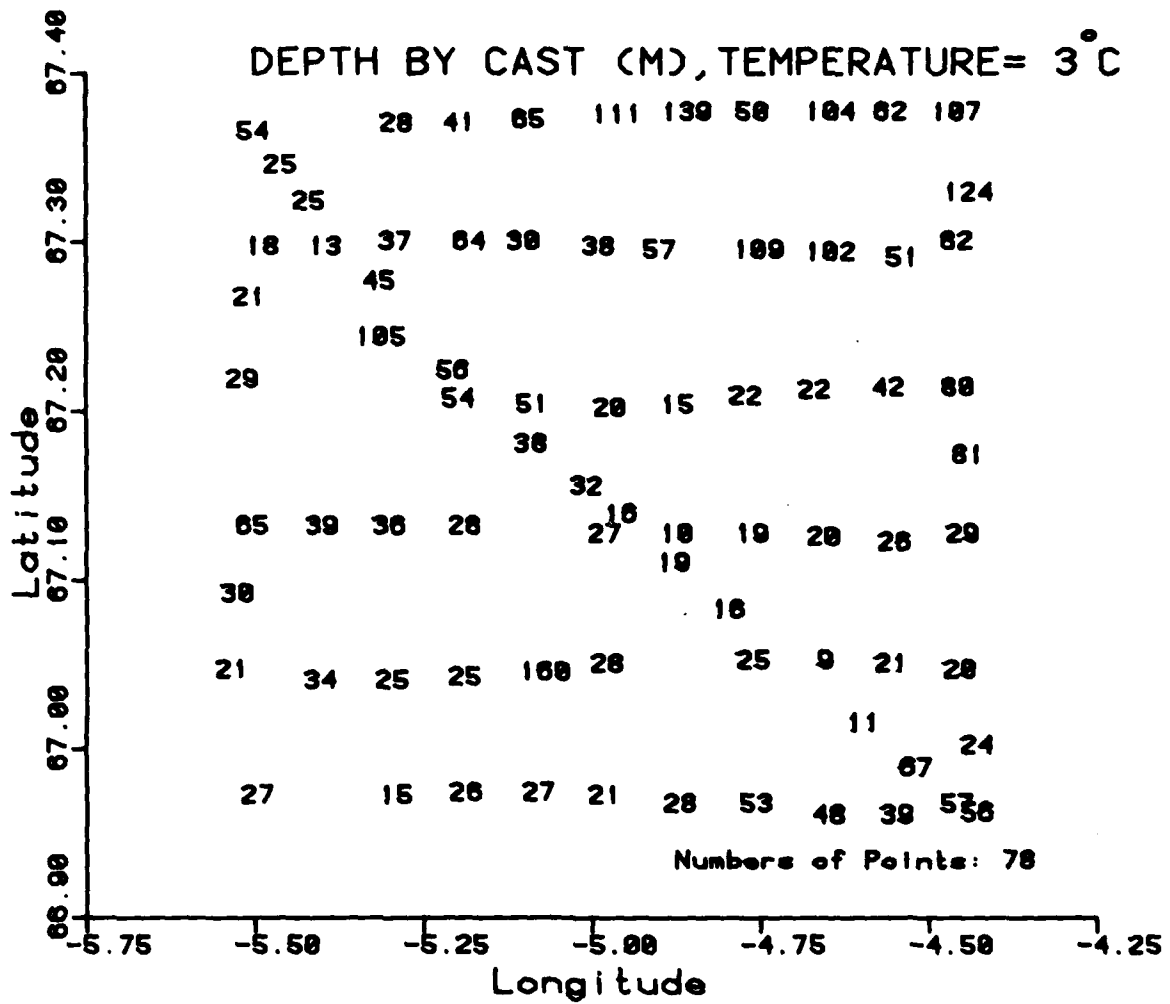


Figure 2 d)

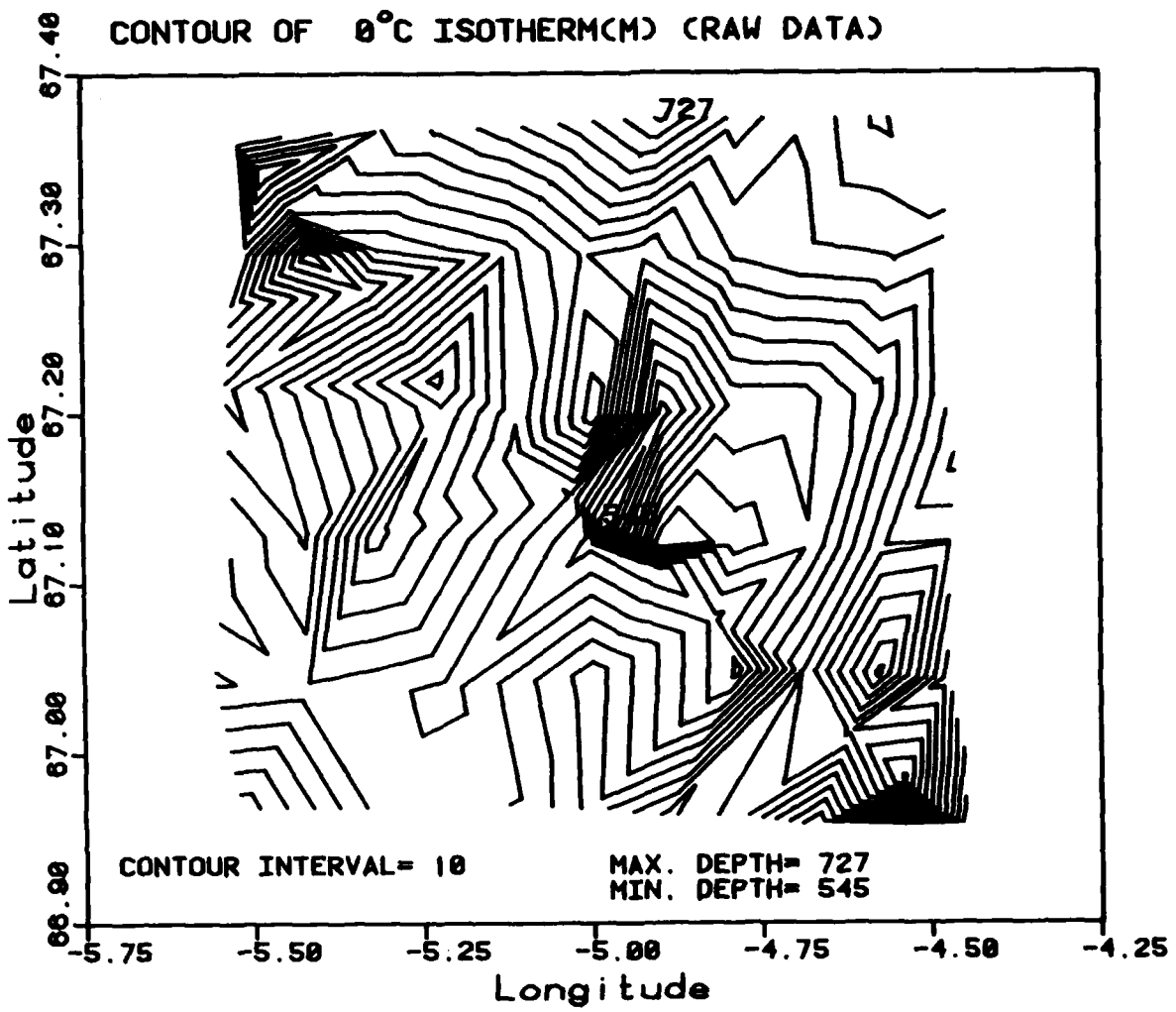


Figure 3 a)

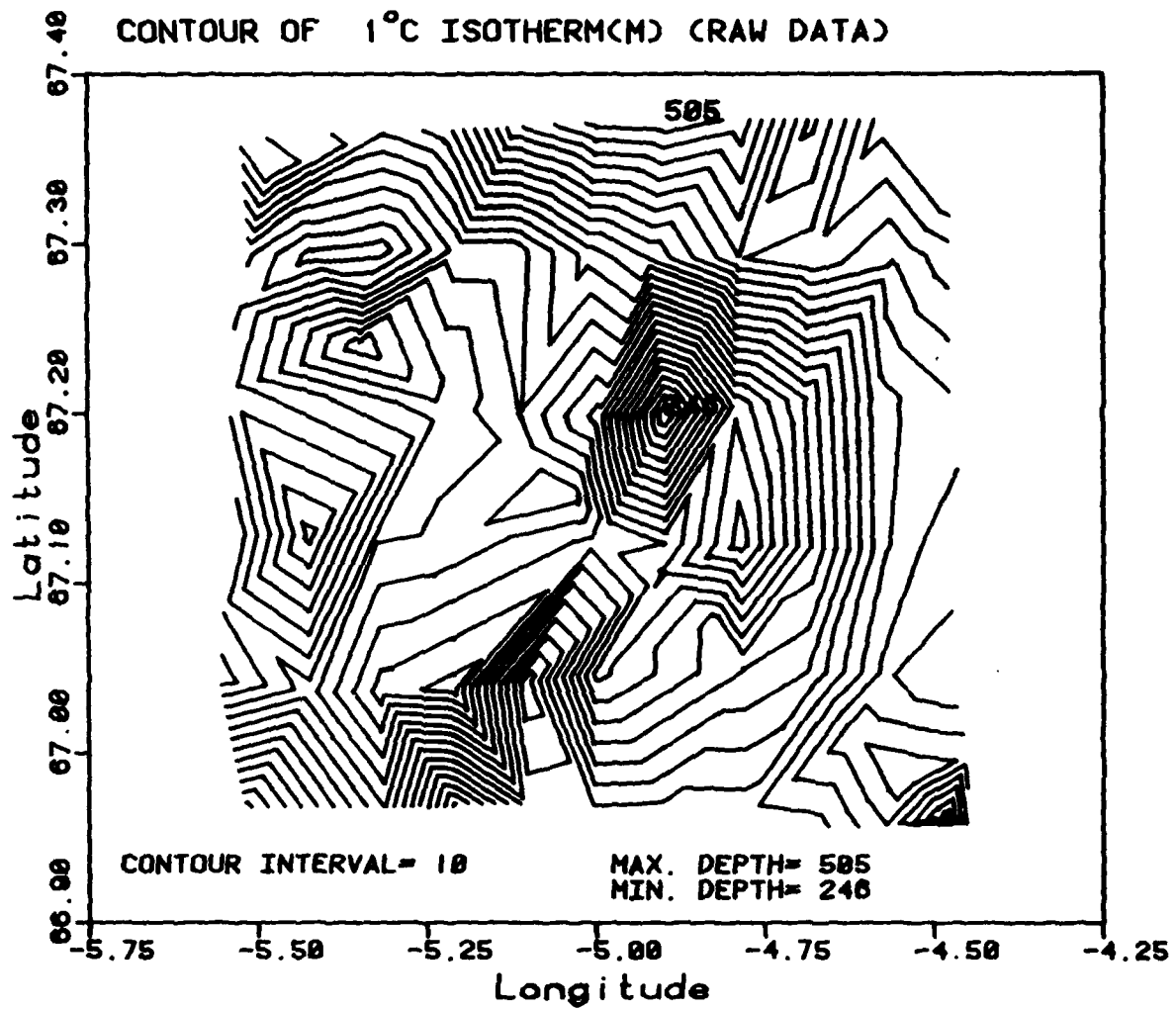


Figure 3 b)

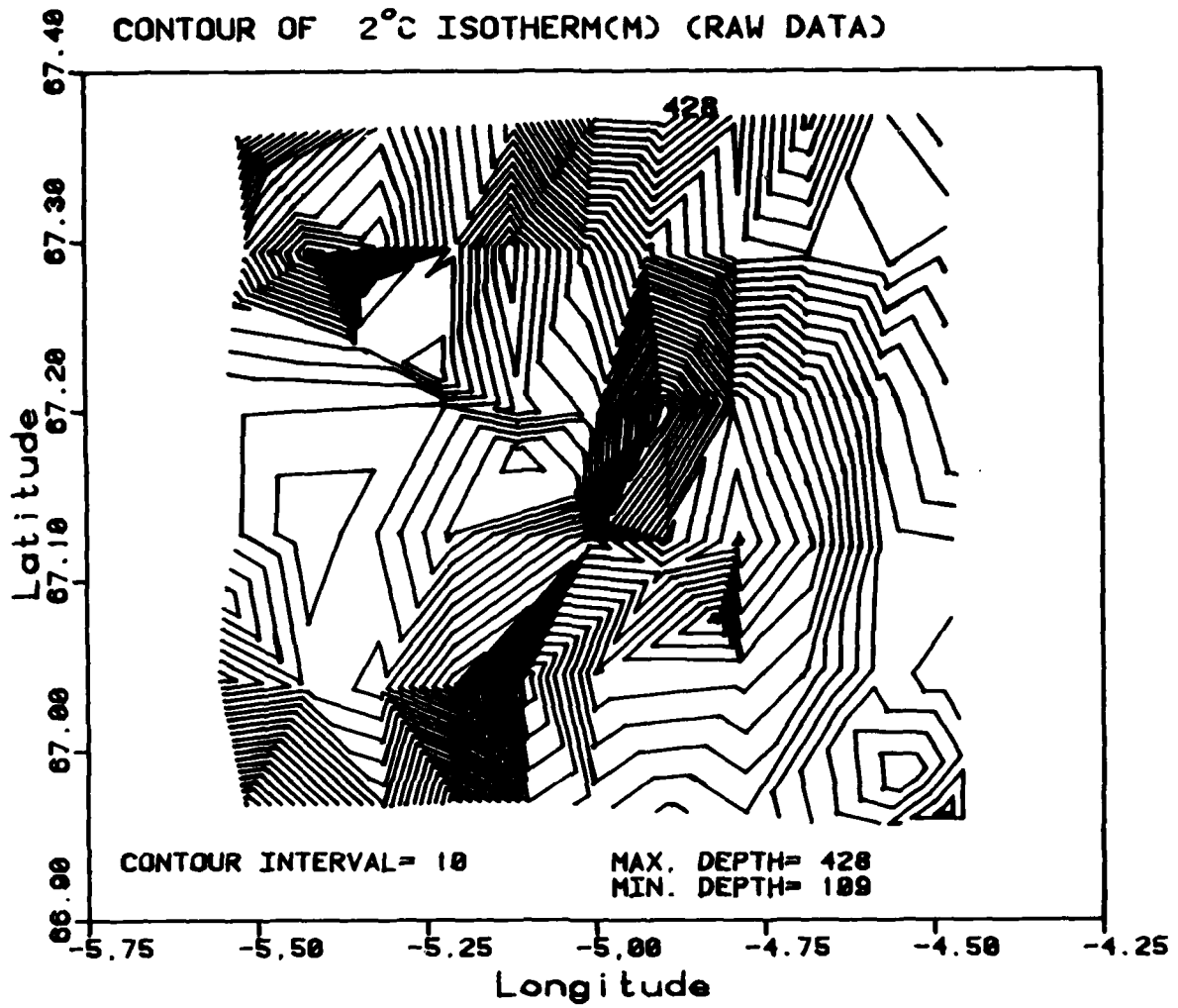


Figure 3 c)

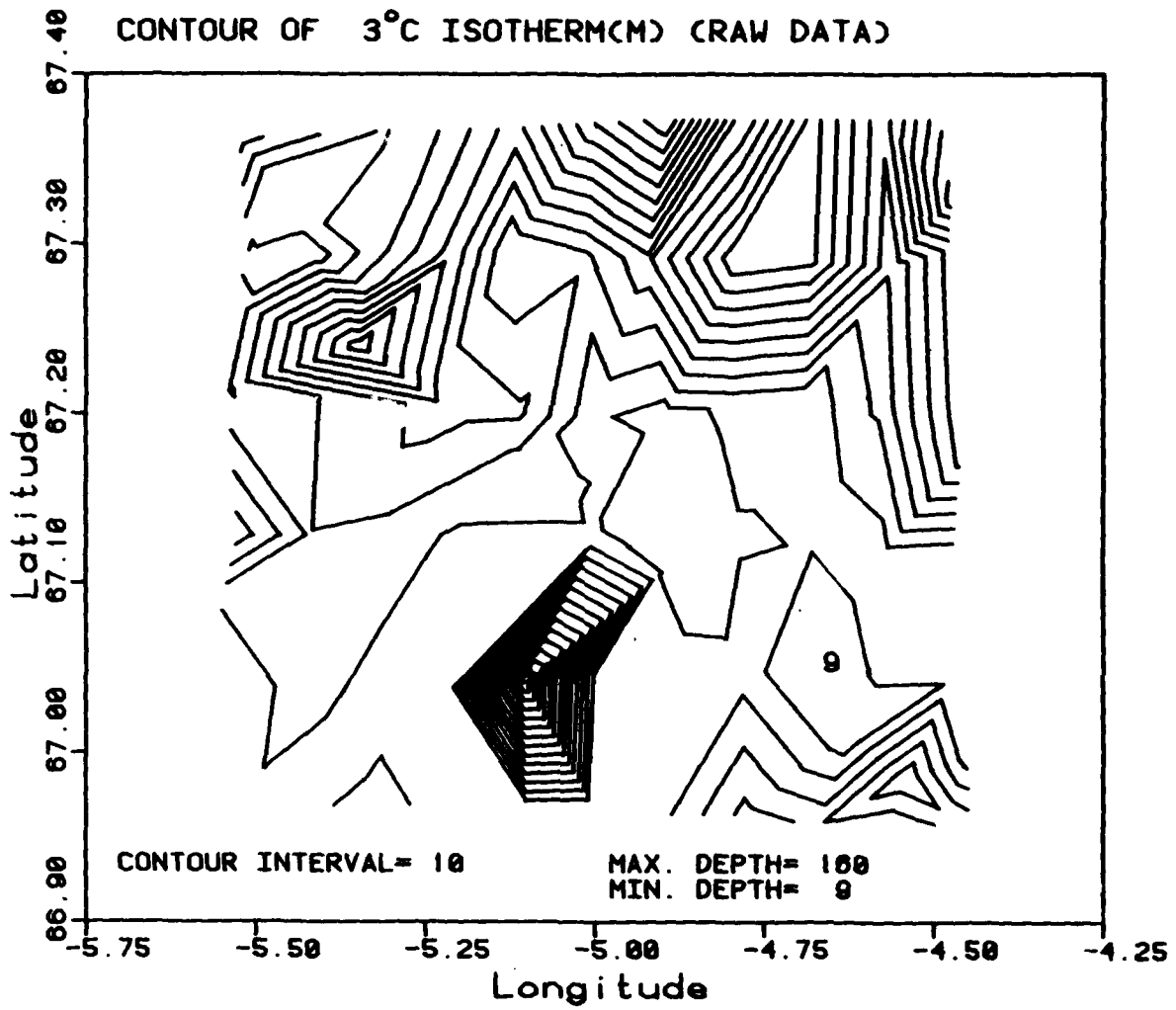


Figure 3 d)

than of ocean dynamics, and attaching geophysical relevance to them would be incorrect.

CONSIDERATION OF ERRORS IN MEASUREMENT

In this section, we begin to deal with the last question posed above: How good are our estimates? To answer this question we must first ask: How good are the data? That is our topic here.

XBTs are simple measuring devices whose reliability is not above reproach. Only two parameters are measured: a voltage corresponding to temperature, and time. The desired variable, temperature as a function of depth, must be inferred. The basis for making this inference is an empirical equation that relates depth to time. The accuracy of this equation, along with its applicability on any given cast, determines how well measurements reflect the actual water column.

We list some of the possible types of errors:

- 1) Systematic errors in depth inference--the time-depth equation is wrong.
- 2) Random errors in depth inference--field conditions alter the time-depth relationship, e.g., high surface waves or large horizontal velocity shears within the water column; manufacturing differences that affect the time-depth relationship differently for each XBT.
- 3) Systematic errors in temperature inference--the temperature bridge circuit is not correctly calibrated.
- 4) Random errors in temperature inference--variability in temperature bridge components; partial shorting of the temperature circuit, e.g., bad sea-water ground or imperceptibly abrading the wire along the ship.

These errors can be classified into two groups: errors in the independent variables--position and time; and errors in the dependent, or measured, variable--temperature. In most experiments the independent variables are accurately known, and it is the error associated with the dependent variable that is of interest. In fact, virtually all of the field of experimental statistics focuses on how to treat errors in the dependent variable. Almost none of it deals with errors in the independent variable. Insofar as the time-depth relationship for XBTs is suspected as being a principal source of error, our problem with measurement error is unusual.

To complicate matters further, our final interest is not in temperature itself, but rather in the depth at which a particular temperature occurs. Here, any error in the measured variable--temperature--will introduce additional errors into our already suspect estimate of depth.

We can model the effects of all these errors with the following equation. Let z^* be the depth at which a given temperature T is measured. Then

$$\delta z = a + bz^* + R + \frac{1}{\left. \frac{dT}{dz} \right|_{z^*}} \delta T$$

where δT is the error in measured temperature and δz is the resulting error in inferred depth. This equation describes a simplified, overall error in the estimate of the depth at which a given temperature occurs. Systematic components (coefficients "a" and "b") are assumed to consist of a constant offset plus a bias proportional to depth. The heaviest contributor to these components are errors in the time-depth relationship, and could easily have a more complex form. The random components have two forms. The first, R , is simple. It has just a characteristic variance (zero mean). It is associated with possible depth-inference errors due to field conditions or XBT variability. The second is much more problematic. Produced by temperature-measurement errors (for whatever reason), this random error consists of a characteristic variance (identified with the temperature-measurement error) divided by the local vertical temperature gradient. The net result is that this component of the error could be without bound. Recall that we are interested in finding the depth at which a given temperature is found. If the temperature measurement is slightly wrong and there is no vertical temperature gradient over, say, 200 meters; then our depth estimate could be off by that much. What makes this component particularly awkward is that the error depends on the measurement itself and so must be accounted for individually for each XBT cast.

Because the depth error may depend on the measurement itself, there is no way we can deduce the statistical properties of its distribution of possible values--not even its mean or variance. We can say that the random portion of the error is uncorrelated between probes. Other than this qualitative statement we cannot say much more. But we need to have an operational definition of error. We could estimate the coefficients of each of the terms, but our estimates would be only guesses. Rather, we will make the oversimplification that the error is a simple random variable with zero mean and constant variance. And this constant variance is just a percentage of the measured variance.

SPATIAL AND TEMPORAL CORRELATIONS OF ISOTHERM DEPTHS

As suggested earlier, in order to properly estimate isotherm surfaces from field experiments, one must collect data in a time short compared to its characteristic time for change, and with a spacing small compared to the lengths of its smallest spatial features. One way to determine whether this criterion is satisfied for a given data collection scheme in a given area is to investigate the space/time correlations of the field. In our case, the only way to infer these correlations is to deduce them from the data.

There are, in fact, two separate questions: What are the temporal correlations of the isotherm fields, and what are the spatial correlations of the isotherm depths over time and at a fixed location. The latter could be obtained by obtaining samples of an isotherm depth at all locations at the same time. Neither of these sampling schemes was used in obtaining the present data set. Consequently, we must improvise.

First, we make the assumption that the field is statistically stationary in time and statistically isotropic in space. That is, the space-time correlation function that we will try to estimate will depend only on separation, and not at all on absolute location. This assumption is necessary because there are too few observations to estimate a more complex function.

Because of the data-taking path of the ship, there are several cases in which data were taken at almost the same place but at different times (refer to Fig. 1). These all occur because the long diagonal track was crossed by the half-dozen horizontal tracks. We found nine pairs of casts which were nominally from the same

location, and calculated the absolute depth differences between the measured isotherm depths. These differences were then normalized with respect to the total root-mean-square (rms) variation of the field. (See Table 1 for rms variations in the isotherm surfaces.) Figure 4(a-d) plots the results as a function of separation in time. These scatter plots are related to what we are interested in--the temporal correlation of the isotherm fields. The normalized mean square depth difference is one minus the correlation.

There are too few observations to make reliable estimates of the temporal correlation functions of our fields, but we can assess them qualitatively. Unfortunately, there appears to be little correlation (i.e., large depth differences) in the isotherm fields at even the smallest differences in time--0.2 days. This implies that whatever time-scale exists for the fields, it is smaller than 0.2 days. In these plots a normalized depth difference of 1.0 means that there is as much variation between the pair of observations as the average variation over the whole field. We cannot be absolutely sure that there is no temporal correlation over the few pairs of observations because the casts were not taken at exactly the same location and, as discussed earlier, the possibility of error in the measurement exists. But the data do not support the hope that the field was "frozen" over the duration of sampling the field.

The next issue--that of determining the spatial correlations of the isotherm fields from the data--now becomes more difficult. Our data were not obtained synoptically, and consequently contain time as well as space differences. That the field was changing rapidly in time confounds our efforts to estimate the effect on correlation due to spatial differences. Figure 5(a-d) shows hybrid, space-time correlation estimates. They are hybrid because, although the abscissas are labeled as kilometers (km), the separations are really both in time and space. Each 10-km spatial difference also includes approximately a .02-day temporal difference. These correlations are calculated in two different ways. Each considers data in segments, a segment being those data obtained in a single, straight ship path. There are seven segments: the six constant-latitude paths and the one diagonal one. Within each segment all possible pairs of observations were used, their separations being grouped by 5-km intervals. The results of all the segments are combined to yield the plots--the numbers indicating how many pairs of casts went into each 5-km interval. Note that for large separations the number of contributing pairs is small.

The two ways of carrying out the calculations have to do with how the data were normalized. In one case, the isotherm depth fluctuations were extracted from the mean isotherm plane of the entire field (see Table 1). In the other, they were extracted from the mean isotherm plane--actually, the mean isotherm line--of their individual segment.

The in-principle difference between these normalizations is to define fluctuations with respect to spatially local vs. global mean isotherm levels. Here, however, in addition to the spatial attribute, the difference includes temporally local vs. distant mean isotherm levels.

Which procedure is more applicable in our case is not evident. On the one hand, our interest is an estimated spatial correlation function over the whole field. On the other, this estimated function should be calculated from data taken as closely together in time as possible. Our evaluation of the temporal correlation suggests that time differences as small as 0.2 days significantly change the field. Do we elect to make calculations on individual data segments collected locally in time and

NORMALIZED DEPTH DIFFERENCE BETWEEN SELECTED PAIRS OF CASTS

TEMPERATURE= 0°C

Pair No.	Casts
1	361, 440
2	362, 441
3	366, 435
4	367, 420
5	368, 421
6	370, 408
7	372, 407
8	374, 400
9	370, 401

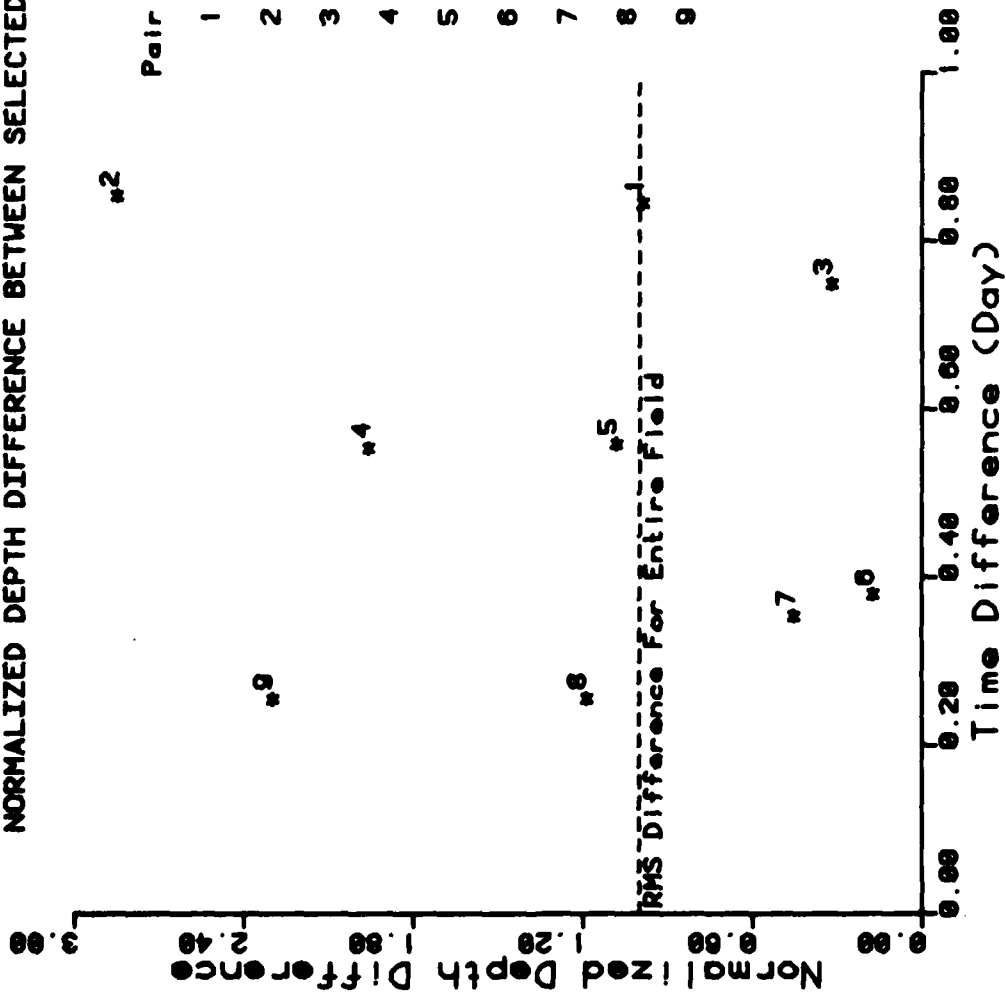


Figure 4 a)

NORMALIZED DEPTH DIFFERENCE BETWEEN SELECTED PAIRS OF CASTS

RMS Difference For Entire Field ----- TEMPERATURE= 1°C

Pair No.	Casts
1	361, 440
2	362, 441
3	366, 435
4	367, 420
5	368, 421
6	370, 408
7	372, 407
8	374, 400
9	376, 401

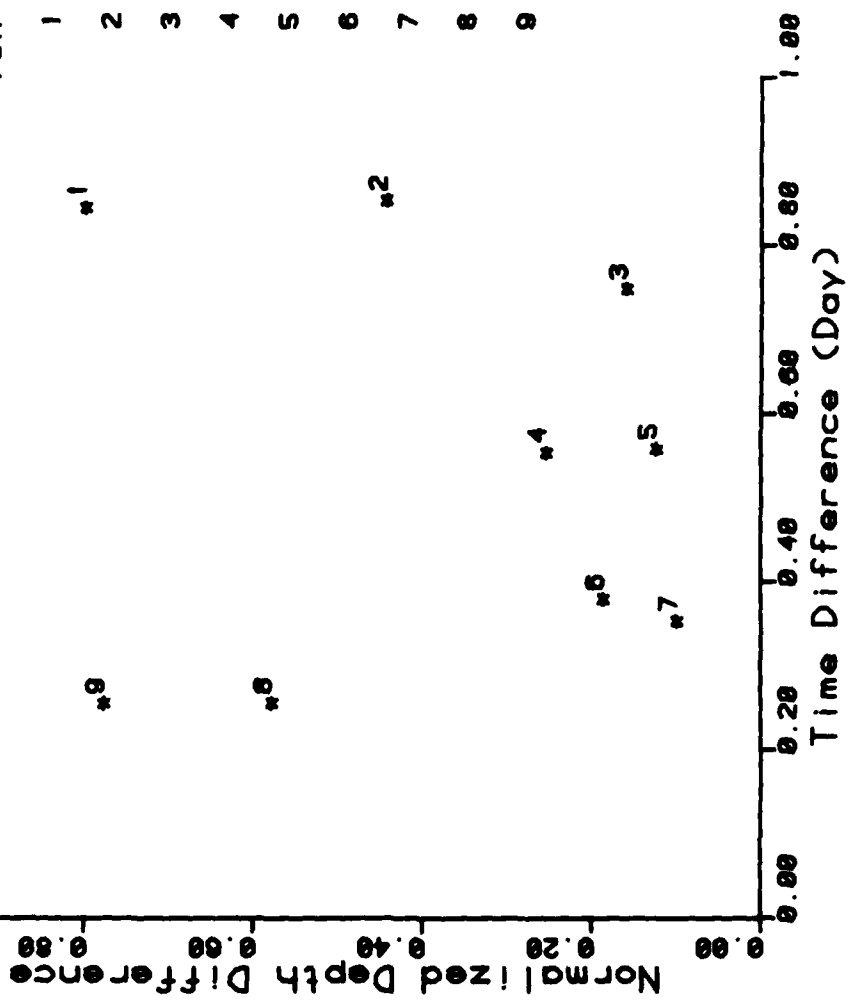


Figure 4 b)

NORMALIZED DEPTH DIFFERENCE BETWEEN SELECTED PAIRS OF CASTS

TEMPERATURE = 2°C

Pair No.	Casts
1	361, 440
2	362, 441
3	366, 435
4	367, 420
5	368, 421
6	370, 408
7	372, 407
8	374, 400
9	376, 401

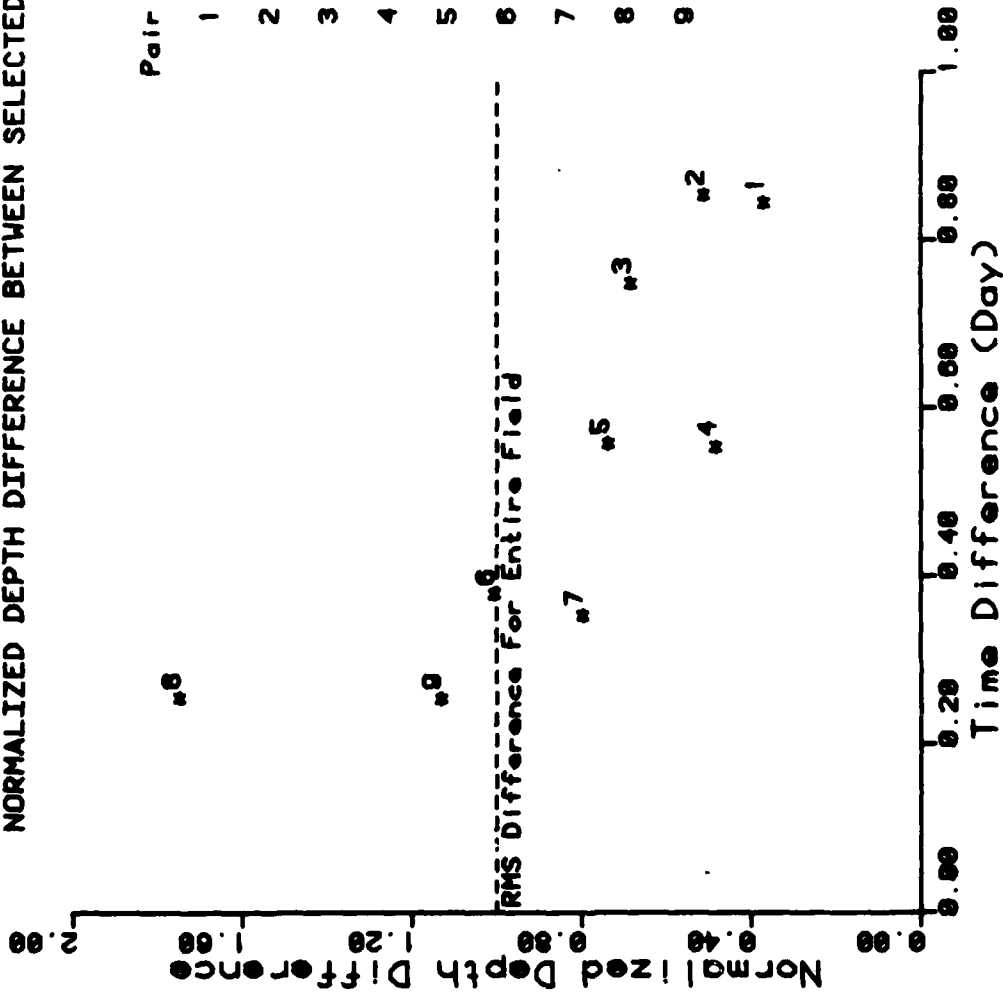


Figure 4 c)

NORMALIZED DEPTH DIFFERENCE BETWEEN SELECTED PAIRS OF CASTS

RMS Difference For Entire Field ----- #2 ----- TEMPERATURE = 3°C

Pair No.	Casts
1	361, 440
2	362, 441
3	366, 435
4	367, 420
5	368, 421
6	370, 408
7	372, 407
8	374, 400
9	376, 401

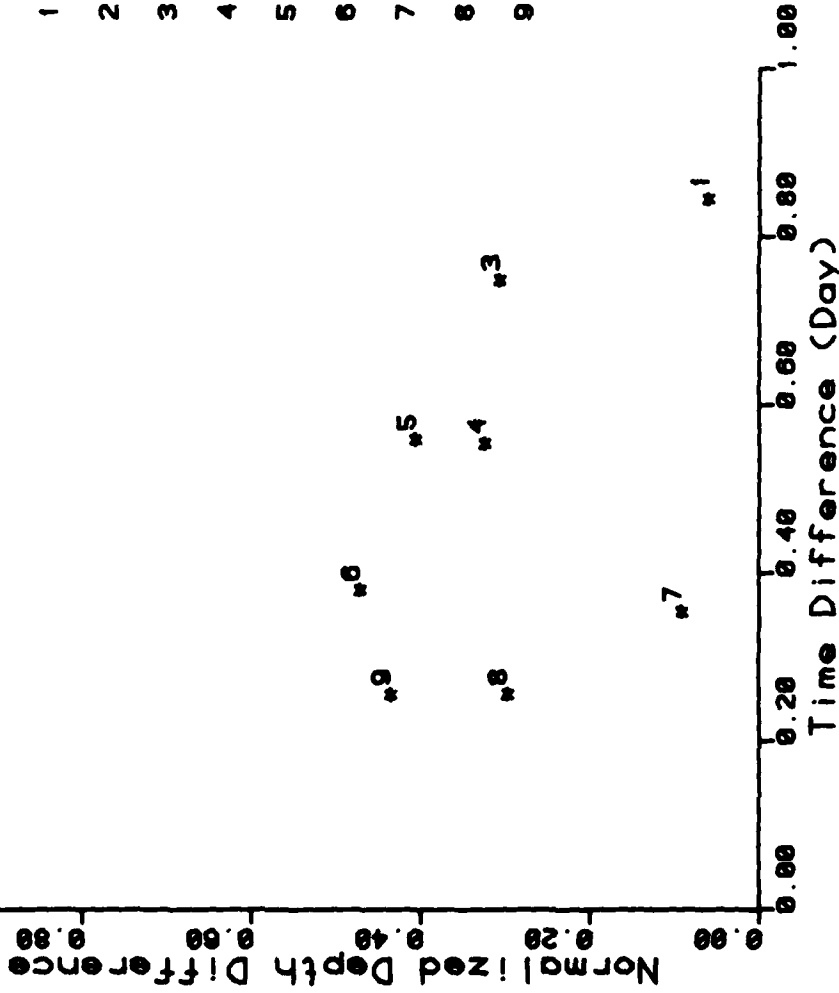


Figure 4 d)

CORRELATION OF DEPTH FLUCTUATIONS BY SEPARATION IN SPACE/TIME

TEMPERATURE = 0°C

— Normalized with respect to single segment
 ---- Normalized with respect to entire field

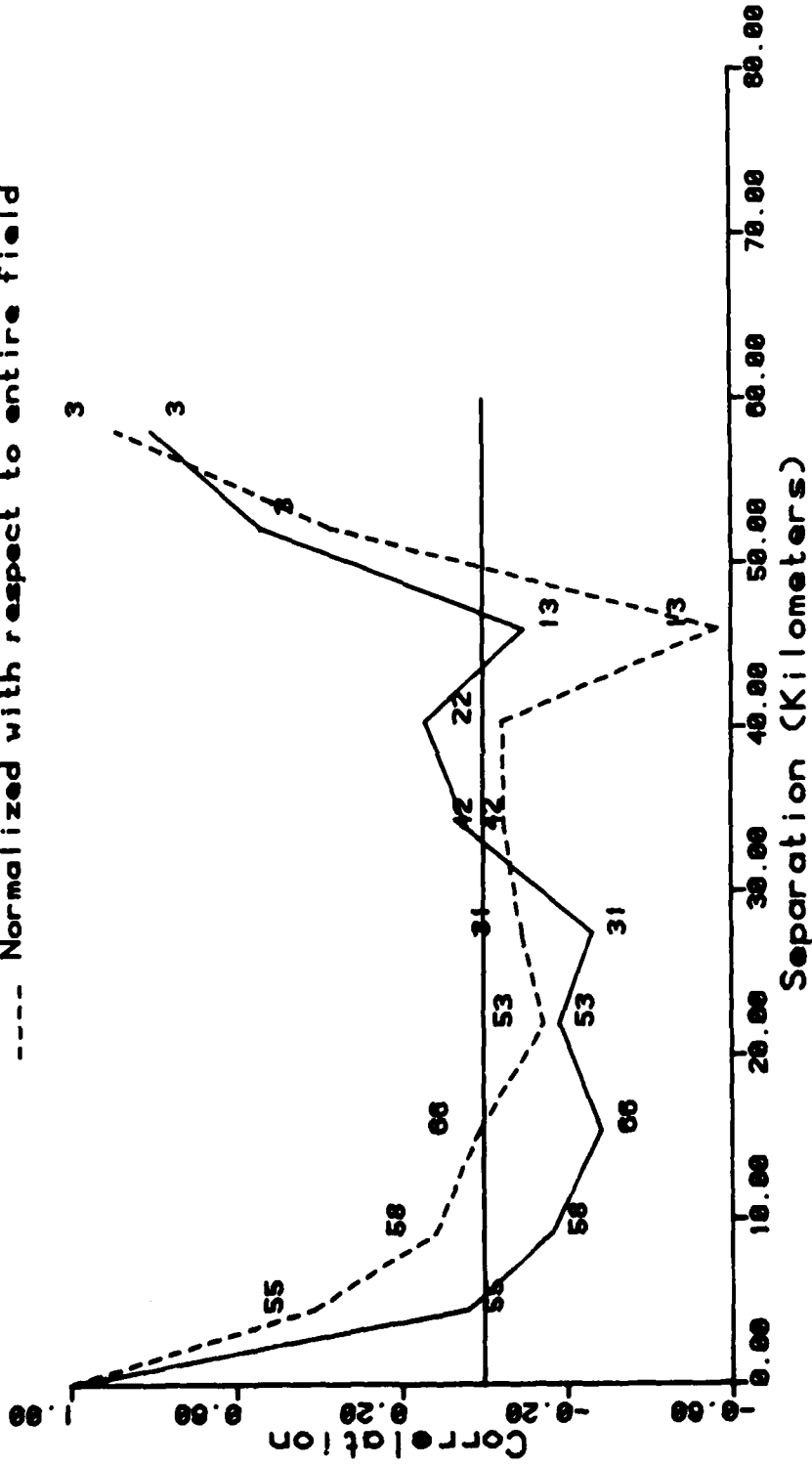


Figure 5 a)

CORRELATION OF DEPTH FLUCTUATIONS BY SEPARATION IN SPACE/TIME

TEMPERATURE = 1°C

— Normalized with respect to single segment
 - - - Normalized with respect to entire field

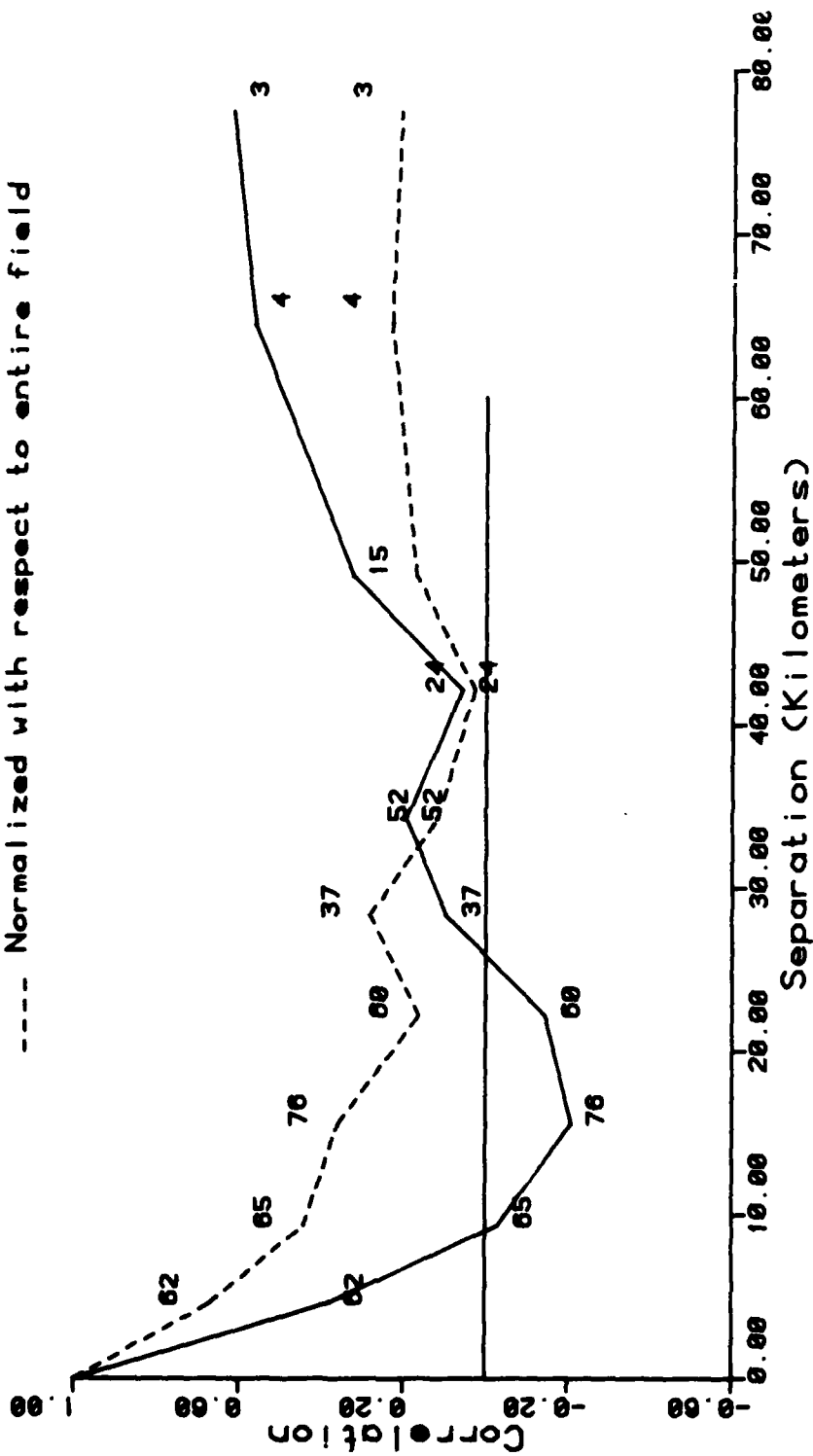


Figure 5 b)

CORRELATION OF DEPTH FLUCTUATIONS BY SEPARATION IN SPACE/TIME

TEMPERATURE= 2°C

- Normalized with respect to single segment
- - - Normalized with respect to entire field

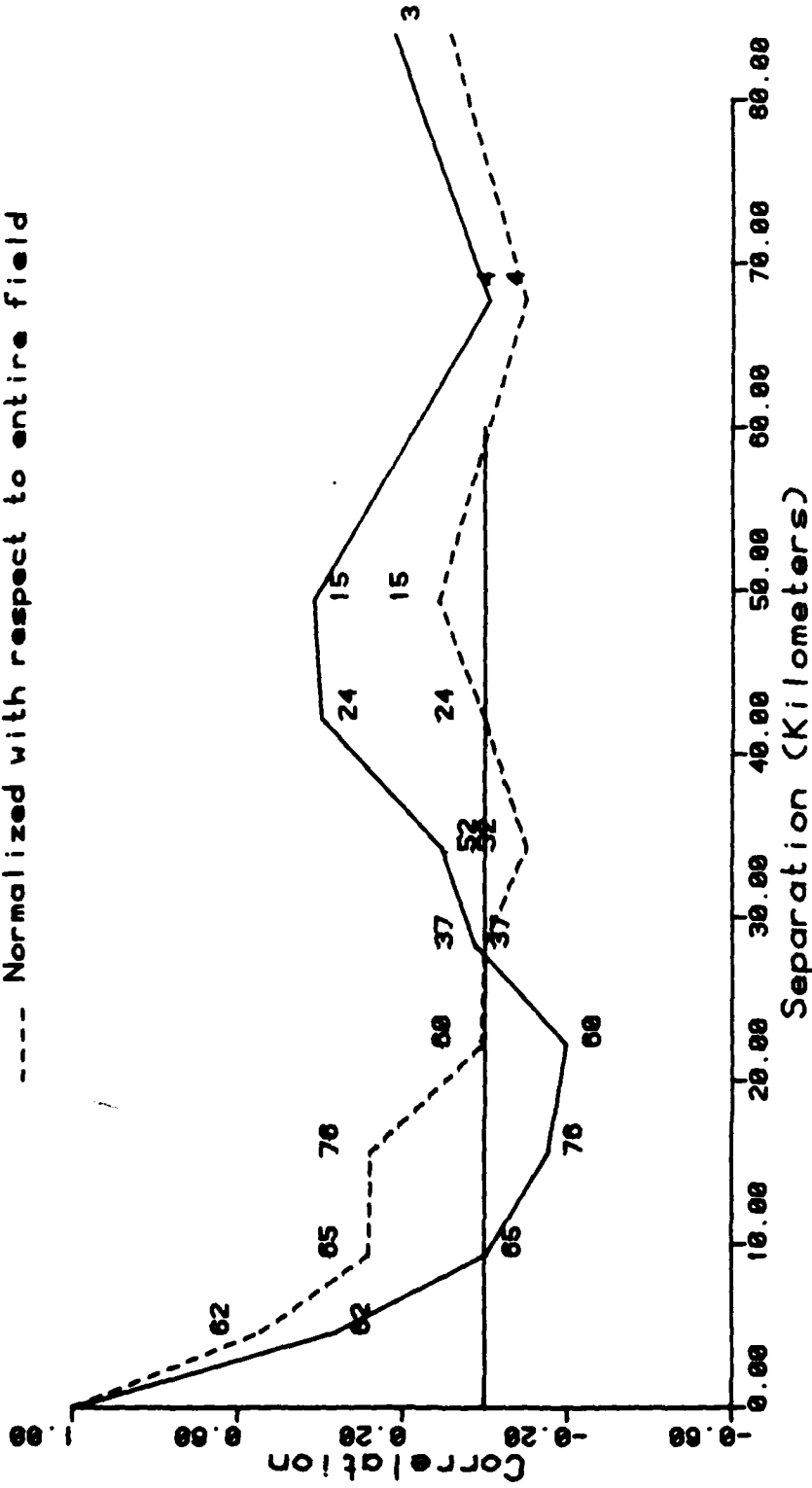


Figure 5 c)

CORRELATION OF DEPTH FLUCTUATIONS BY SEPARATION IN SPACE/TIME

TEMPERATURE= 3°C

- Normalized with respect to single segment
- - - Normalized with respect to entire field

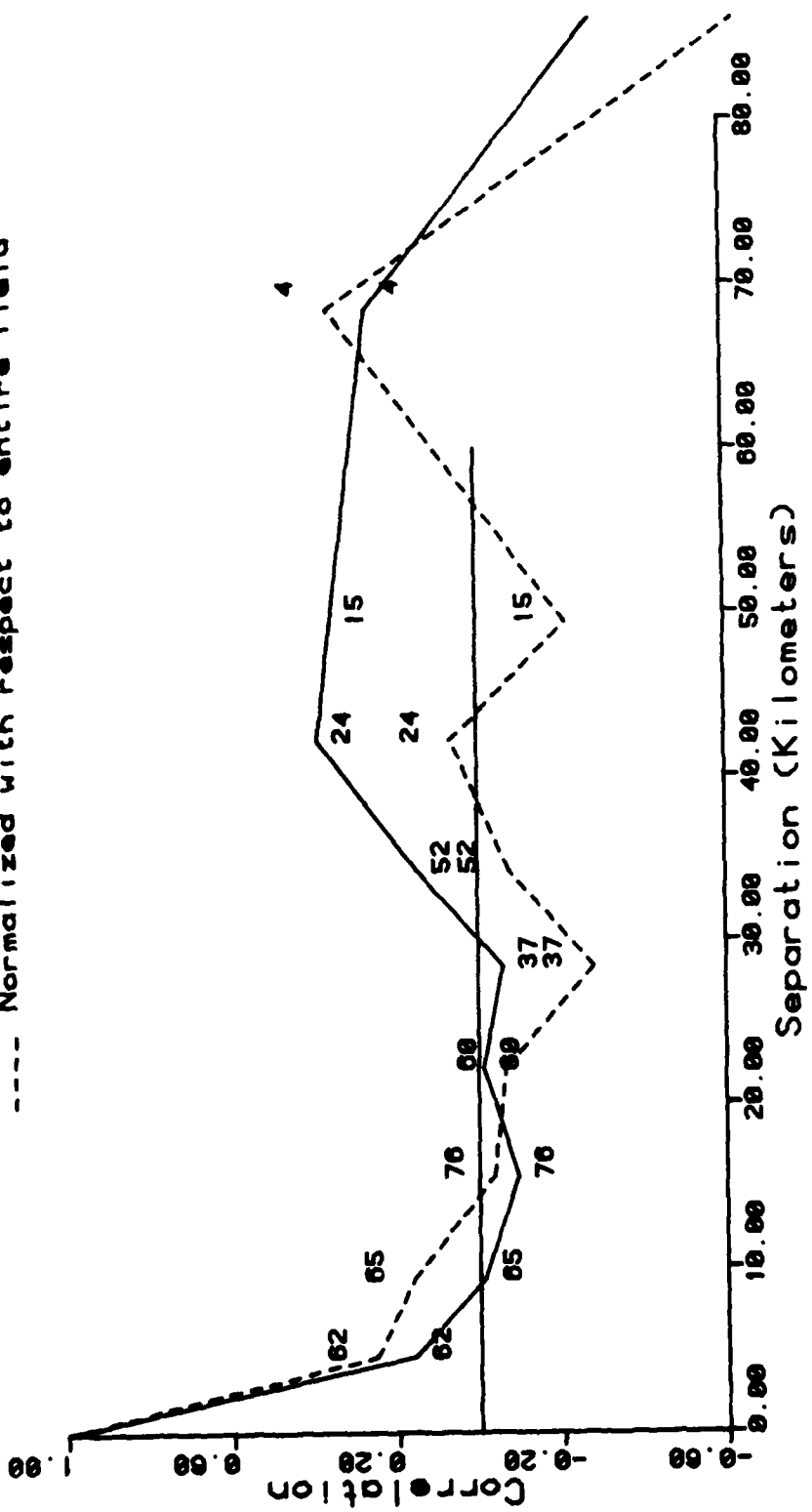


Figure 5 d)

ignore the variation in the field between the segments or do we elect to make calculations on data from the whole field and ignore the field's changes over time?

Figure 5(a-d) shows the results from both approaches. Note that the estimated correlations from the global normalization are larger than those estimated from the segment normalization. This is so because a significant part of the correlation using a global normalization comes from correlated segment depths. When one normalizes with respect to segment depths, that correlation is removed and the resulting correlation is reduced.

The most striking result is that for the segment normalization, the spatial correlation drops to zero for all of the temperatures with a separation of about 10 km. If one temporarily ignores the confounding time difference, this says that the current data set sampled the spatial features of the isotherm field only about twice per feature--not nearly enough to obtain accurate spatial statistics. Again, interpretation of these calculations must be made cautiously because of an unknown contribution from nonlinear, depth-measurement errors.

The final blow to making justifiable inferences about the spatial scales of these isotherm fields is what we just ignored--the time difference between the spatial measurements. If the time-difference calculations carried out earlier are even partially reflective of the true dynamic nature of the field, then spatial surveys by ship are not possible in these sections of the ocean. And so our initial goal of producing maps of isotherm surfaces in this area cannot be met.

Are there other ways of interpreting our calculations? First, we have alluded to a number of problems involving the measuring instruments themselves--the XBTs. The lack of correlation could be the result of very poor XBT casts. Table 1 shows the results of reducing the data set to mean isotherm planes and residual variations. Note that at all temperatures, there is nominally a 1 m/km downward slope of the mean plane toward the north and toward the west. Note also, that the rms depth fluctuation $[3'2]^{1/2}$ at each temperature is only about 40 meters.

The accuracy of the inferred depth for XBT casts is quoted by the manufacturer as a percentage of that depth. Even at an error of two percent, if it is random, the depth uncertainty at 500 m depth would be 10 m. In a field whose measured rms isotherm-depth fluctuation is only 40 m, who is to say what is physical and what is measurement error? This alone could account for poor space/time correlations.

Second, in carrying out our calculations we tacitly assumed that the field was statistically constant in both space and time. "Events" such as fronts or local internal currents could have violated that assumption. In such a case, averaging over the whole field to obtain stable statistics would be inappropriate, and we could expect distorted correlations.

There is no way of determining the answer from these data.

ISOTHERM MAPPING

We have concluded that the present data set cannot justifiably be used to estimate isotherm surfaces for this area. The distance between sample points was too far to obtain the required spatial resolution, and the time to collect the data was too long to render the field frozen.

Nevertheless, we will produce isotherm maps. This will not be done for evaluating the characteristics of the sampled field, but rather for illustrating several techniques for producing them and for demonstrating hypothetical interpretation problems when appropriate field data are considered.

The process of producing maps from scattered data has two parts. One is estimating the behavior of the field between the data points--interpolation. The other is accounting for potentially poor observations. In any mapping procedure, each of these parts plays an important role in the final estimate of the map. Often the mapping technique itself automatically encouches both parts.

In what follows we offer isotherm maps from three different processing procedures: linear interpolation of raw data, surface approximation by Fourier analysis, and surface approximation by objective analysis.

Linear interpolation of raw data is more of a display of data than of an analysis scheme. Here, the field is divided up into contiguous triangular segments whose vertices are the positions of the collected data. Each triangle is assumed to be planar, so the depths of the vertices completely determine the level and "tilt" of that triangular segment. Isotherm depths become line segments within each triangle and are contiguous across triangle boundaries. Interpolation is linear between data, and no consideration is given to possible measurement errors. Figure 3(a-d) shows contour maps from this simplistic method.

Closely spaced contours indicate steep horizontal gradients. Note, especially for the 0-degree isotherm, many of the large gradients occur along the diagonal ship track. This is a feature not of the isotherm field, but rather of the consequences of sampling the field over too long a period. The main diagonal represents the initial ship track that was later criss-crossed in the systematic sampling of the area. Because of the partially redundant survey pattern, in several instances observations were made at almost the same location--but at distinctly different times. Due to the poor temporal correlation of the field, these observations yielded significantly different isotherm depths that here appear as large depth differences over small horizontal distances--hence the large apparent spatial gradients. Cast 432 indicates a tremendous depth anomaly in all the maps for which there were data. Although the temperature profile of this cast looks reasonable by itself, it most likely is a "bad" cast.

The two other mapping schemes that we are about to describe--Fourier analysis and objective analysis--are based on depth fluctuations about a mean isotherm-depth plane, and not on the isotherm depths themselves. This technique eliminates the large constant component associated with each isotherm depth and increases the sensitivity of the analysis to the features relative to that depth plane. Additionally, because the mean plane can be sloped, we can approximately subtract out the very large-scale features that in our sampled area would contribute to the isotherm depth as (almost) linear trends. Procedurally, the mean isotherm-depth plane is calculated and subtracted from the data; the mapping schemes are applied to these depth fluctuations; and the results are displayed with the mean plane added back in. Refer again to Table 1 for the characteristics of the mean plane and fluctuations.

In view of the isotherm-depth decomposition presented in Table 1, we require our mapping schemes to estimate surfaces of depth fluctuations whose rms amplitude is roughly 40 m, measurement error included.

TABLE 1

Isotherm Planes

Variances of observations about isotherm planes

Depth observations for a given temperature were decomposed as

$$z(x,y) = \bar{z} + m_x(x-\bar{x}) + m_y(y-\bar{y}) + z'(x,y)$$

where $\bar{z}, \bar{x}, \bar{y}$ are depth and position averaged over all the observations,

m_x, m_y are mean slopes calculated over all the observations by least-squares,

$z'(x,y)$ are residual depth differences

T(°C)	\bar{z} (m)	m_x (m/km)	m_y (m/km)	$[z'^2]^{1/2}$ (m ²)
0.	636.8	1.04	0.99	34.8
1.	404.9	1.47	0.51	44.9
2.	276.2	1.99	0.91	58.1
3.	45.9	0.58	0.89	28.2

Fourier mapping consists of approximating depth-fluctuation surfaces as linear combinations of sinusoidal oscillations. In our treatment we assume that the isotherm surfaces (with the mean and linear trend removed) are periodically extendible in space in both the longitude and latitude directions. Then this infinitely extended surface becomes representable as a two-dimensional Fourier series. We must make this assumption of periodic extension to justify using Fourier series as a representation of the field. The Fourier-series representation of the depth-fluctuation surface $z'(x,y)$ is then

$$z'(x,y) = \sum_{k=-n/2}^{n/2} \sum_{l=-n/2}^{n/2} \{A_{kl} \cos[2\pi(\frac{kx}{X} + \frac{ly}{Y})] + B_{kl} \sin[2\pi(\frac{kx}{X} + \frac{ly}{Y})]\}$$

where x and y are position coordinates with respect to the principal periodic lengths $X = 45.06$ km and $Y = 50.00$ km--in our case, the dimensions of the sampled area. By performing a least-squares analysis on a truncated series, we can deduce a best Fourier fit to our measured surface. Insofar as there are nominally only 75 casts in our survey, we must truncate this series at $n = 4$. Each term in the series is characterized by the two wavenumbers k, l , and both the amplitude and phase of each term (represented by A_{kl} and B_{kl} in the above equation) must be estimated from the data. A higher wavenumber representation would require more observations for analysis than we have.

Results are presented in two ways. Figure 6(a-d) displays reconstructions of the Fourier-approximated isotherm surfaces. Figure 7 shows the relationship between the Fourier approximations and the data along the ship track. This figure presents all the isotherm interpolations as a function of cast number. (Figure 8 is included to show a Fourier series fit with only three wavenumbers.) Quantitatively, the five-wavenumber-Fourier approximation accounts for 63.7, 71.2, 71.2, 55.6 percent of the surface variations in isotherms 0, . . . , 3, respectively.

The first thing to note is that a truncated Fourier-series approximation is smooth. By allowing only low wavenumbers to contribute to the surface, the more rapid fluctuations (in space) are filtered out. As a result, the effect of bad data in the form of "depth spikes" are minimized. However, this representation also precludes an accurate rendering of sharp fronts that may well be present in the field. In comparing the raw-data contours (Figure 3(a-d)) with the Fourier-produced contours we find significant differences between them. At casts 410 and 432, the depth jumps recorded in the data have been filtered out; at casts 438-442, the Fourier analysis has introduced an additional depression not measured. These differences are manifested by the Fourier surface-approximation scheme. In the former case, the filtering is probably justified because those casts were probably bad; in the latter case, the calculated depressions are probably not justified because the depressions probably did not exist in the field. Again we have no way of knowing, because the correlation between observations is so small that we cannot use other local observations to lend credence to apparently anomalous observations.

Objective analysis is another way of estimating the shape of isotherm surfaces. Whereas the Fourier technique approximates surfaces as a superposition of sinusoidal oscillations and, hence, limits the inclusion of sharp gradients, the objective analysis scheme approximates surfaces as weighted averages of the data and does not preclude such gradients. In fact, this technique is a "best" linear interpolation

FOURIER-APPROXIMATED ISOTHERM CONTOURS

TEMPERATURE= 0° C

MAX. ABS. WAVE NUMBER= 2

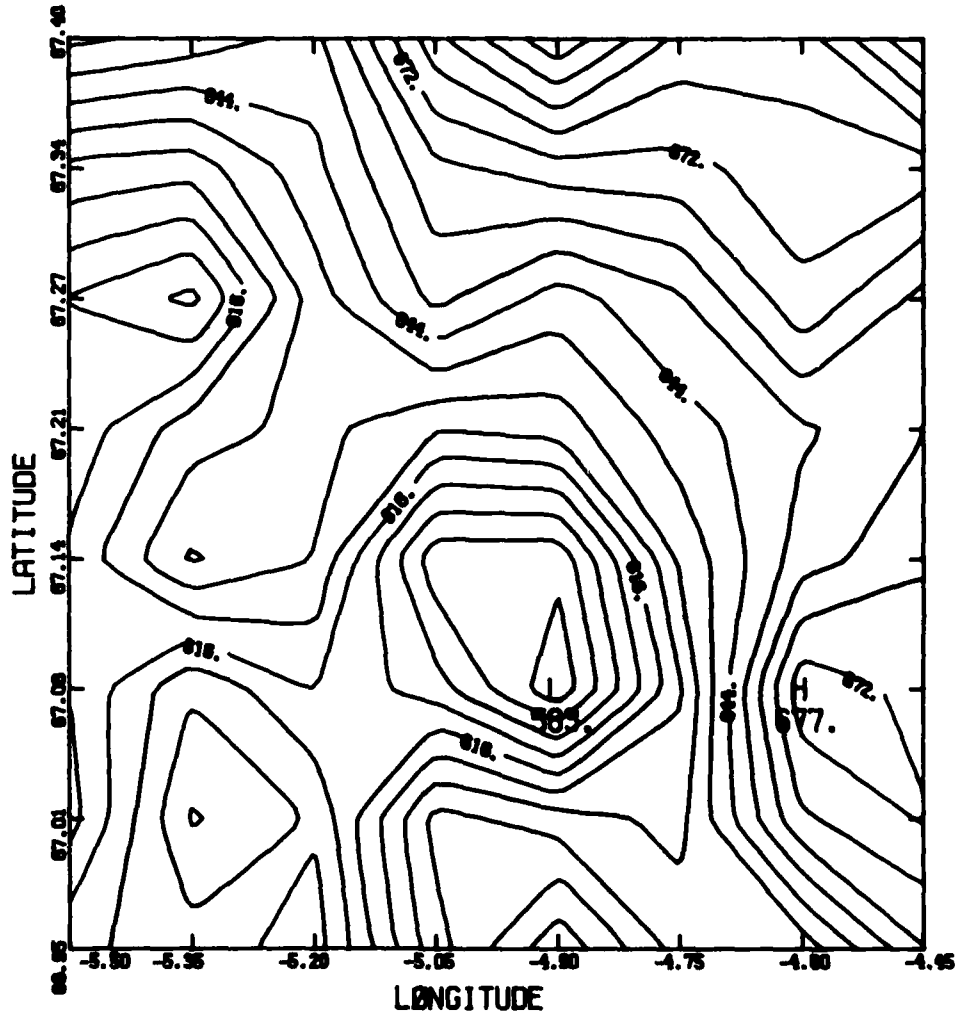


Figure 6 a)

FOURIER-APPROXIMATED ISOTHERM CONTOURS

TEMPERATURE = 1°C

MAX. ABS. WAVE NUMBER = 2

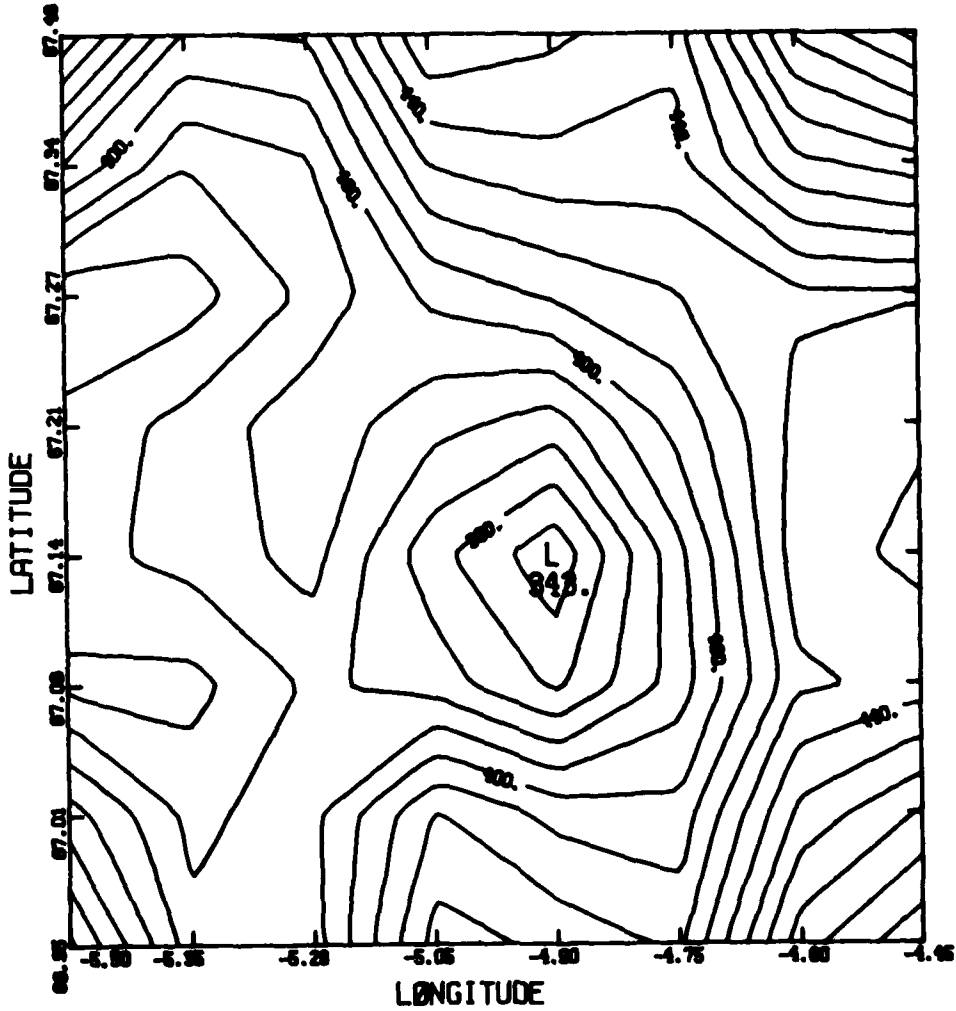


Figure 6 b)

FOURIER-APPROXIMATED ISOTHERM CONTOURS

TEMPERATURE = 2° C

MAX. ABS. WAVE NUMBER = 2

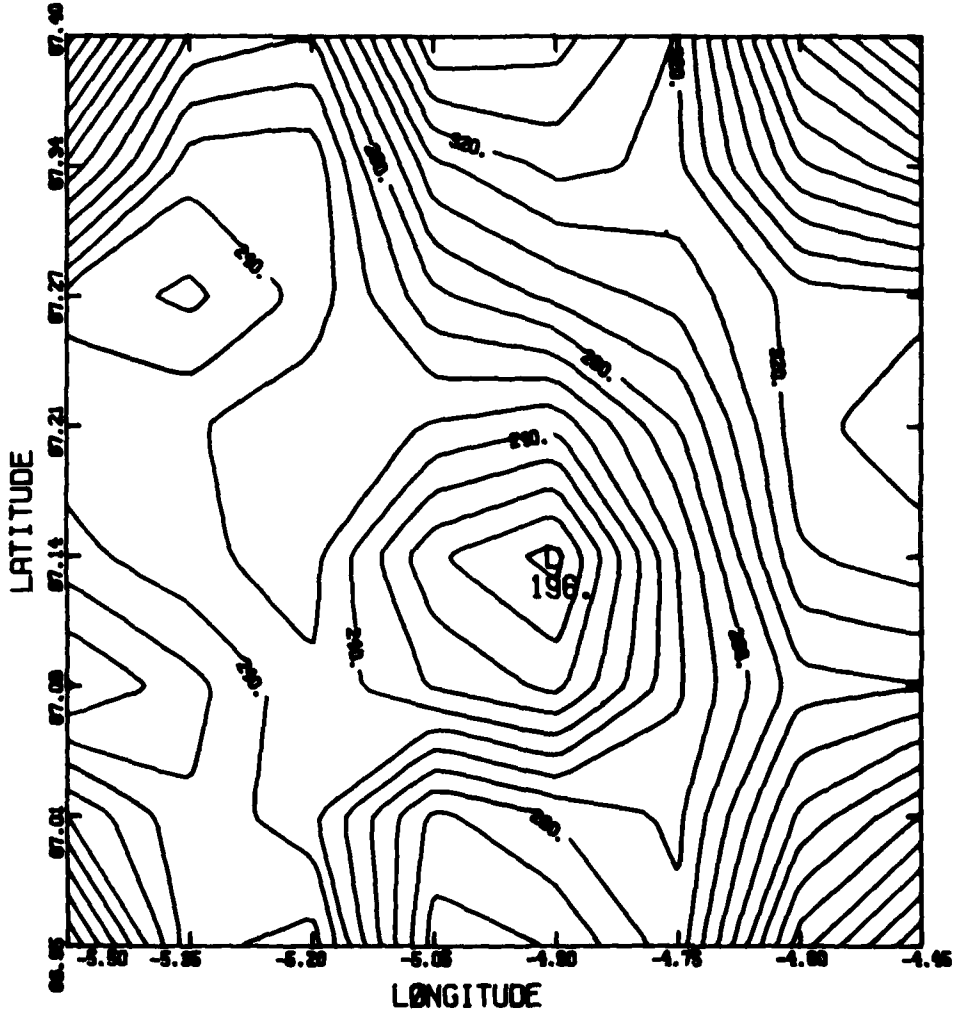


Figure 6 c)

FOURIER-APPROXIMATED ISOTHERM CONTOURS

TEMPERATURE = 3°C

MAX. ABS. WAVE NUMBER = 2

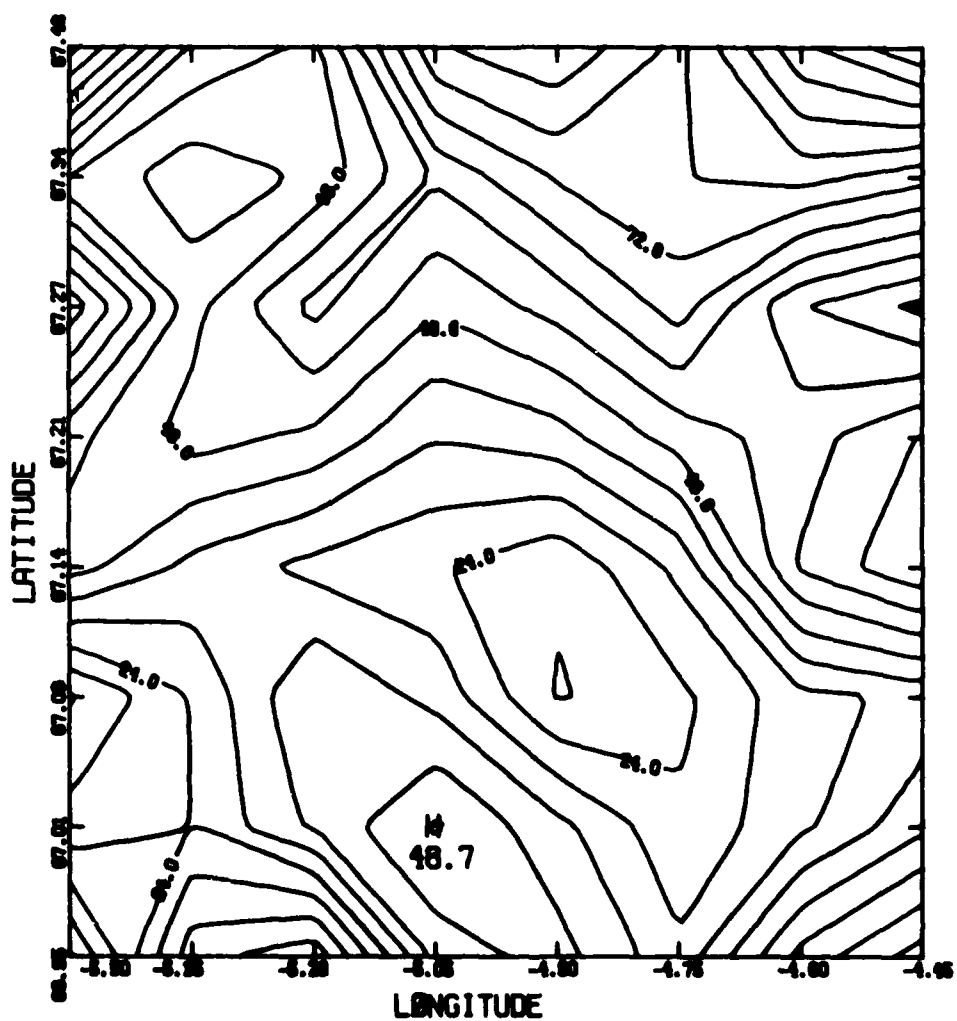


Figure 8 d)

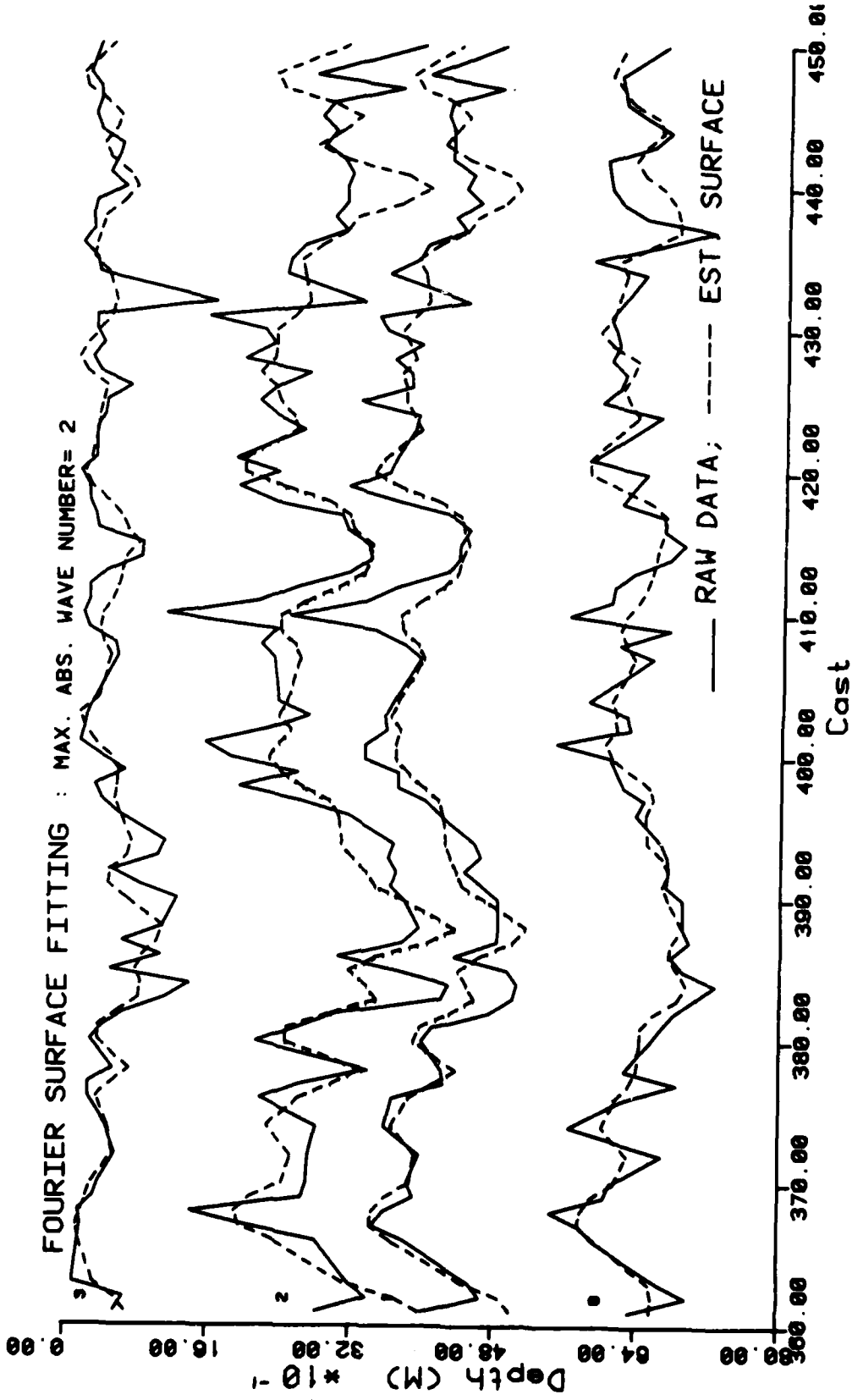


Figure 7

scheme. (Objective analysis was introduced by L. S. Gandin in the monograph "Objective Analysis of Meteorological Fields," Israel Program for Scientific Translation, Jerusalem, 1965. See also, M. Karweit, "Optimal Objective Mapping: A Technique for Fitting Surfaces to Scattered Data" in Advanced Concepts in Ocean Measurements for Marine Biology, University of South Carolina Press, 1980.)

The assumption of objective mapping is that each point in the field may be estimated in terms of a linear combination of the data, the coefficients of which are related to the spatial correlation of the field. The observations contribute to the estimate at the required point depending on their distances to the point. Each contribution is determined by the magnitude of the spatial correlation at that separation.

An additional feature of the technique is that one can assign measurement errors to the observations, either en masse, or individually. Thus data quality can be incorporated into the estimated map.

Usually the objective mapping technique is applied to situations in which observations are highly correlated, and the points of required estimation are local to these observations. In our sampled isotherm fields, however, the spatial correlations drop to zero over very short distances; and some positions where we would like to obtain an interpolated isotherm depth are so far from any data that our observations provide virtually zero information. To obtain anything at all we must use a spatial correlation function whose length scale is greater than that measured. (Recall that our estimated spatial correlation function was contaminated by time differences as well; so that the other difficulties notwithstanding one could justify inflating the measured length scale.)

The objective mapping procedure works most conveniently if the correlation is defined functionally. For that purpose we defined the correlation to be a Gaussian curve with a width (standard deviation) of 6.2 km for all the isotherm surfaces. Also, we arbitrarily assigned a measurement error variance to all observations of 20 percent. Our use of the objective mapping procedure consisted of estimating isotherm depths over a uniformly-spaced, 8 x 8 grid. The final interpolation between the grid point was by one-dimensional splines, under tension.

Figure 9(a-d) shows the results. The presented contours are qualitatively similar to those produced by Fourier interpolation, but they are quantitatively different. They are different for several reasons. First, the objective mapping scheme was not restrictive in accommodating steep horizontal gradients. Second, the objective mapping scheme produced an estimated surface "piece-wise"; that is, each estimated point on the surface was determined by data local to the point. In the Fourier technique, data contributed to the amplitude and phase of oscillations that spanned the entire field. So an anomalous observation could influence the isotherm depth estimate at a far away point. Third, there was no a priori error variance assignable to the Fourier representation, as there was to the objective analysis mapping. In the Fourier technique, there is a de facto error assignment associated with ignoring contributions to the surface of higher wavenumber oscillations; but this error assignment is based on differences between observations, not on the observations themselves.

A by-product of objective analysis is a procedure for producing an error map; that is, a map of the expected error in the estimated isotherm surface. Recall that the estimated depth at each point on the surface is assumed to be a weighted, linear

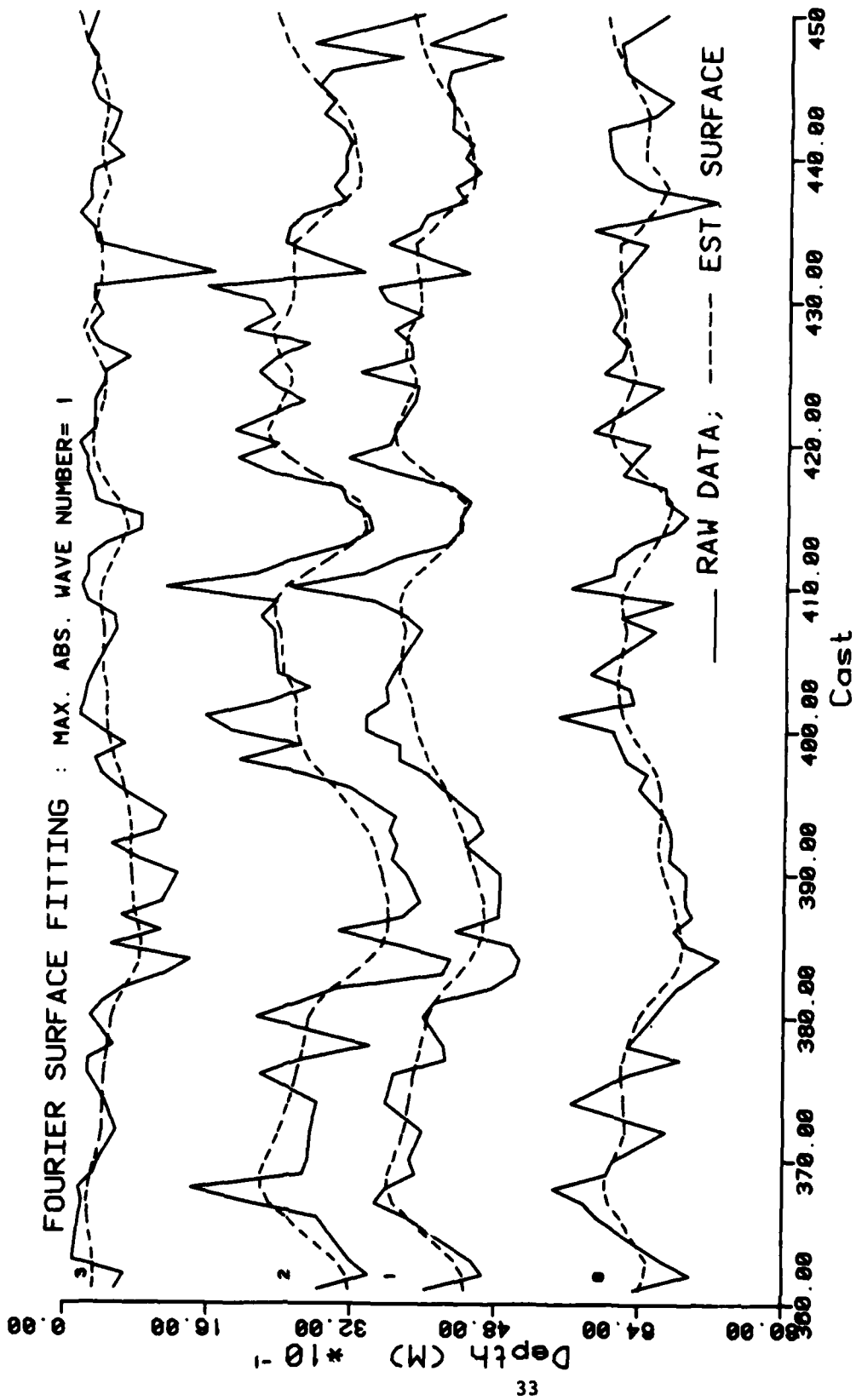


Figure 8

OBJECTIVE MAPPING ISOTHERM CONTOURS

TEMPERATURE= 0° C

ERROR VARIANCE= 0.2000

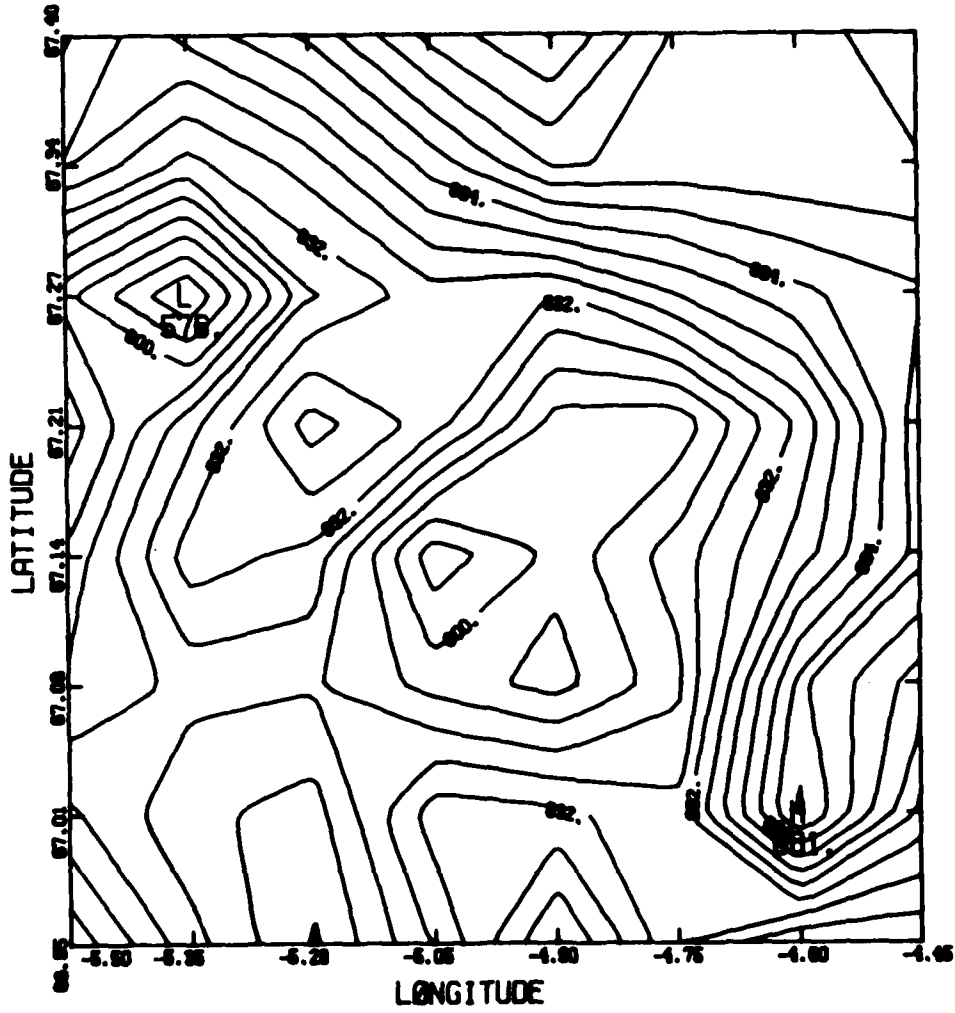


Figure 9 a)

OBJECTIVE MAPPING ISOTHERM CONTOURS

TEMPERATURE= 1°C

ERROR VARIANCE= 0.2000

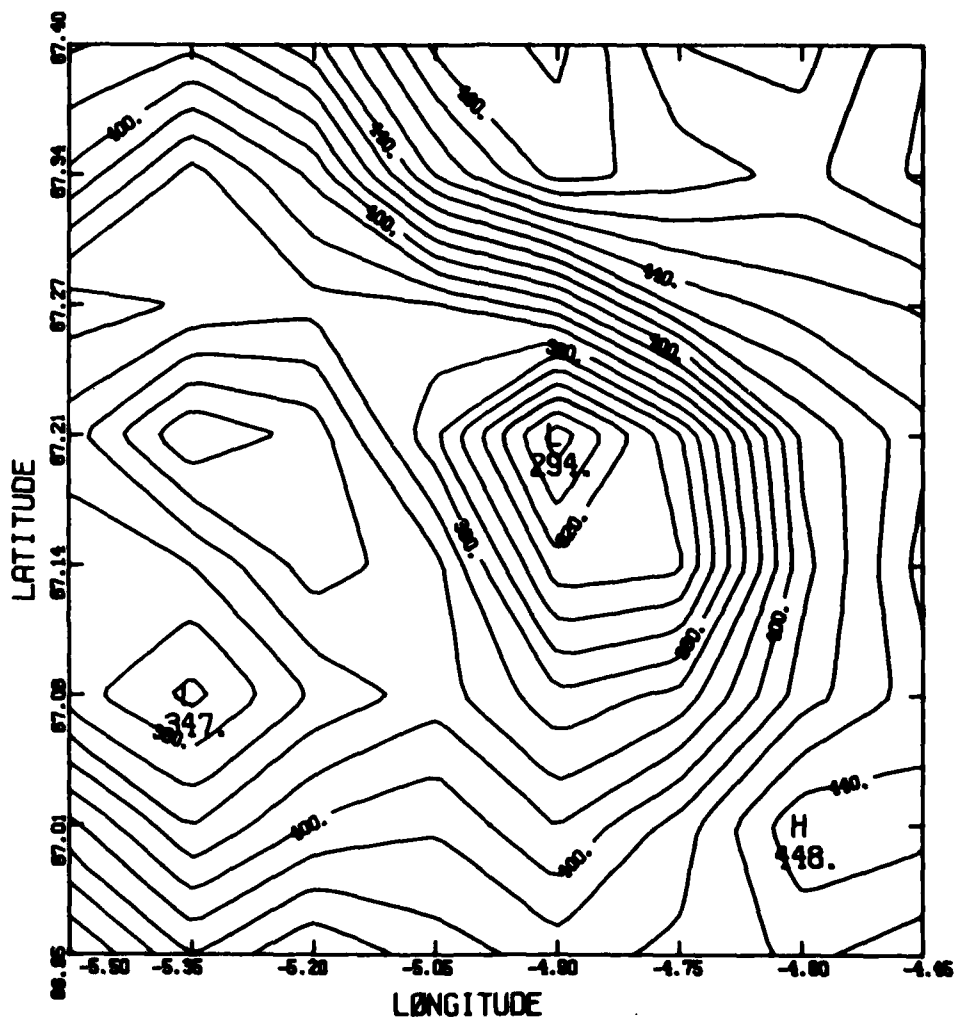


Figure 9 b)

OBJECTIVE MAPPING ISOTHERM CONTOURS

TEMPERATURE= 2° C

ERROR VARIANCE= 0.2000

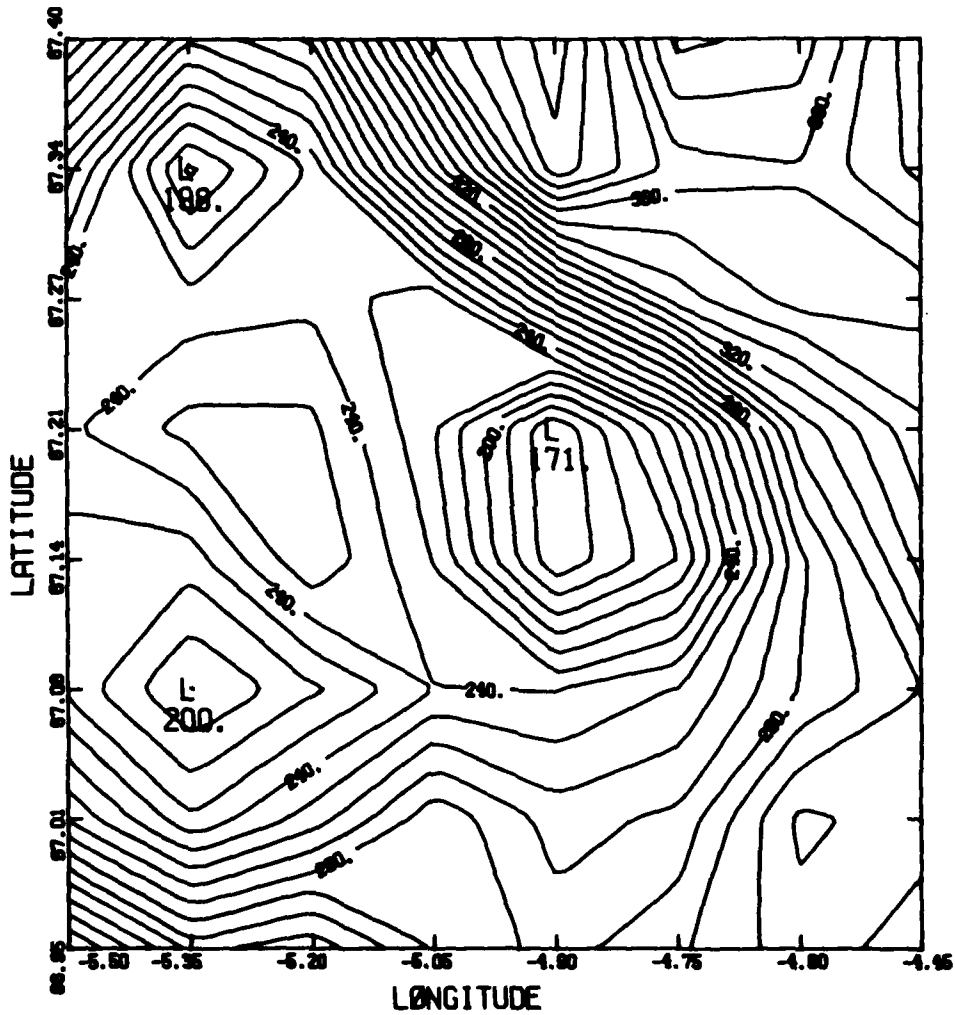


Figure 9 c)

OBJECTIVE MAPPING ISOTHERM CONTOURS

TEMPERATURE= 3°C

ERROR VARIANCE= 0.2000

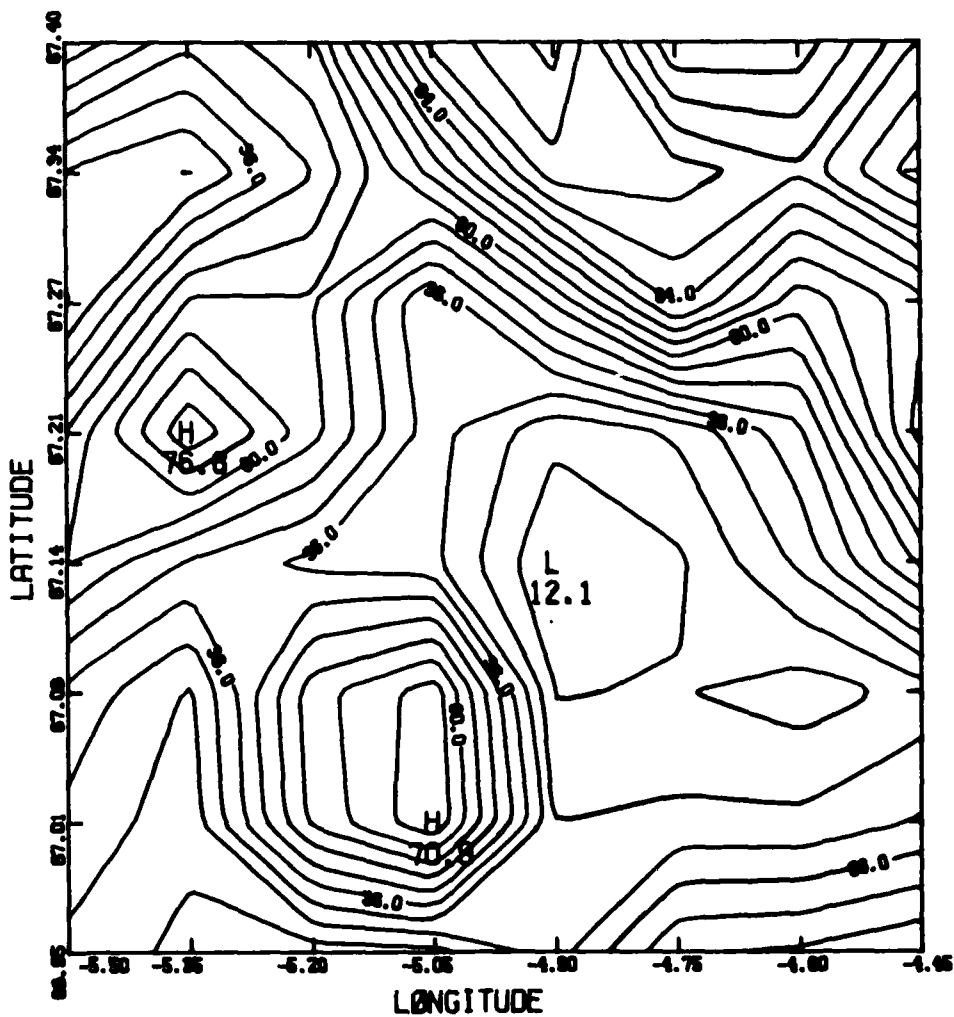


Figure 9 d)

combination of the observations--the weights being related to the spatial correlation function. Since both the observations and the attached weights can be in error we would like to be able to estimate their impact on our estimate. This was carried out using the procedure detailed in the above-mentioned Gandin and Karweit monographs. Results for our isotherm surfaces are given in Figure 10(a-d).

In principle, the objective mapping technique is "best." That is, it can be shown that the technique yields the least mean-square error of all possible linear methods. And since the Fourier scheme is a linear method, it is subsumed by objective analysis. However, there are reasons why one might want to consider Fourier analysis as a means of estimating isotherm surfaces: measurement errors are incorporated into the estimated fields in a different way; functional descriptions of the fields are automatically obtained; and, the coefficients of the Fourier terms indicate the contribution of the various length scales to the isotherm surfaces. It is only after one decides for what purpose the field will be analyzed that one can decide on the most appropriate field approximation strategy.

Because the data, and consequently the interpolated surfaces, do not represent a valid description of an actual field (for reasons already described) we do not offer an oceanographic interpretation to our results.

CONCLUSIONS

In this work we have tried to do two things: develop a methodology for inferring isotherm fields from shipborne observations; and, applying that methodology, interpret an XBT data set obtained in a section of ocean in the Norwegian Sea. We have partially succeeded only in the first goal. Insofar as our methodologies are statistical, they require certain properties of the field. That these exist for the field and that their quantities be estimated can only be deduced from an appropriate experiment. In the present case, data were collected through such an experiment--perhaps the best that one can hope for from a single ship. Unfortunately the survey was not adequate to capture the features of that particular segment of the ocean. The speed of the ship compared to the dynamics of the ocean was too slow to render the collected data as a spatial picture. Each observation being taken deliberately at a different position was also taken at a different time--so much so at a different time, that lack of correlation in the field could never be parceled between the spatial and temporal features of the field.

An additional problem has to do with the measuring instrument itself--the XBT. Potential errors or variations in drop rates affect isotherm-depth interpretations in proportion to those errors or variations. However, potential errors or variations in the measured temperature affect the interpretations in proportion to the inverse of the local vertical temperature gradient. In regions of little or no gradient, the error in the inferred isotherm-depth can be arbitrarily large. Measuring incorrect temperatures is probably not due to manufacturing variations, but rather is probably due to deployment difficulties. In many cases an XBT cast can be discarded as "bad" because of an irregular-looking recorded profile. In some cases, however, the profile looks all right; but the recorded temperature is wrong. (Evidence of this problem was found in an XBT-CTD comparison study carried out by NAVOCEANO. Results were analyzed in a Technical Report by M. Karweit: "An XBT data quality evaluation using CTD casts for comparison," November 24, 1982.) The principal difficulty is an a priori one cannot tell whether a cast is "good" or "bad."

OBJECTIVE MAPPING ERROR MAP

TEMPERATURE= 0° C

ERROR VARIANCE= 0.2000

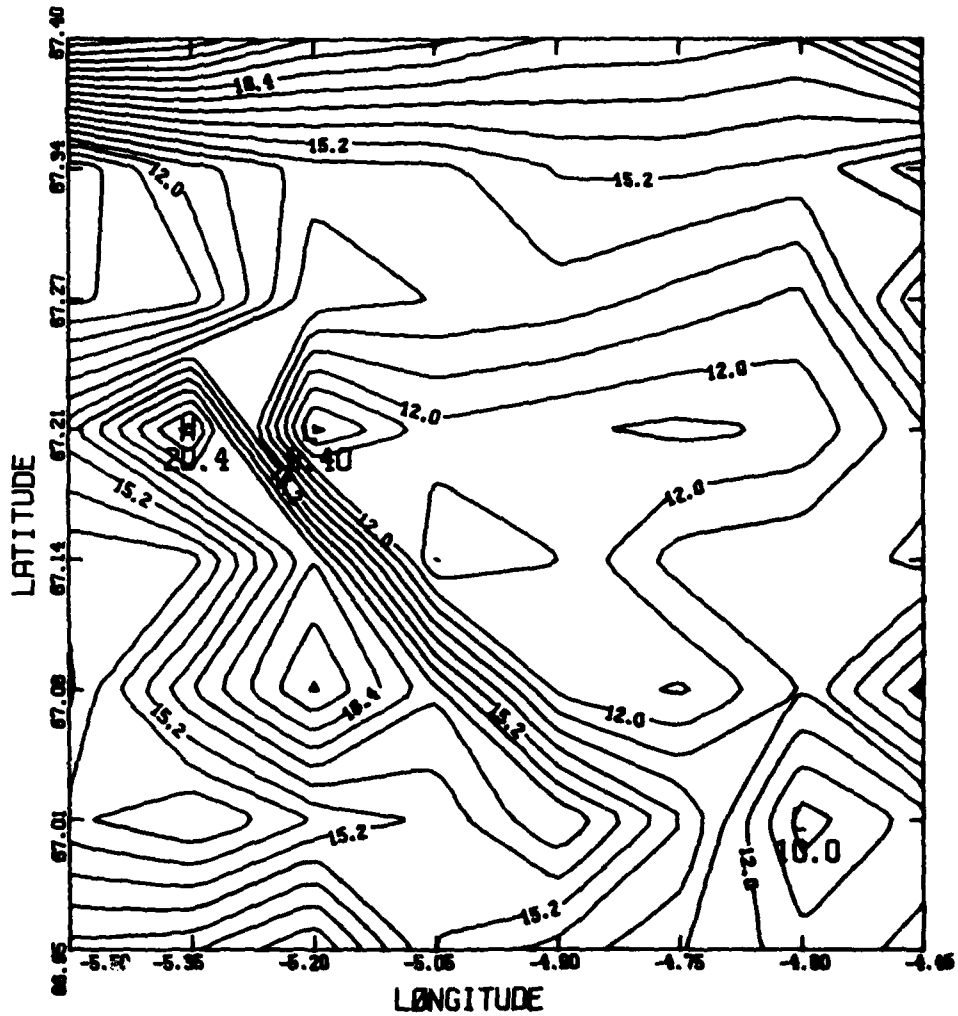


Figure 10 a)

OBJECTIVE MAPPING ERROR MAP

TEMPERATURE= 1°C

ERROR VARIANCE= 0.2000

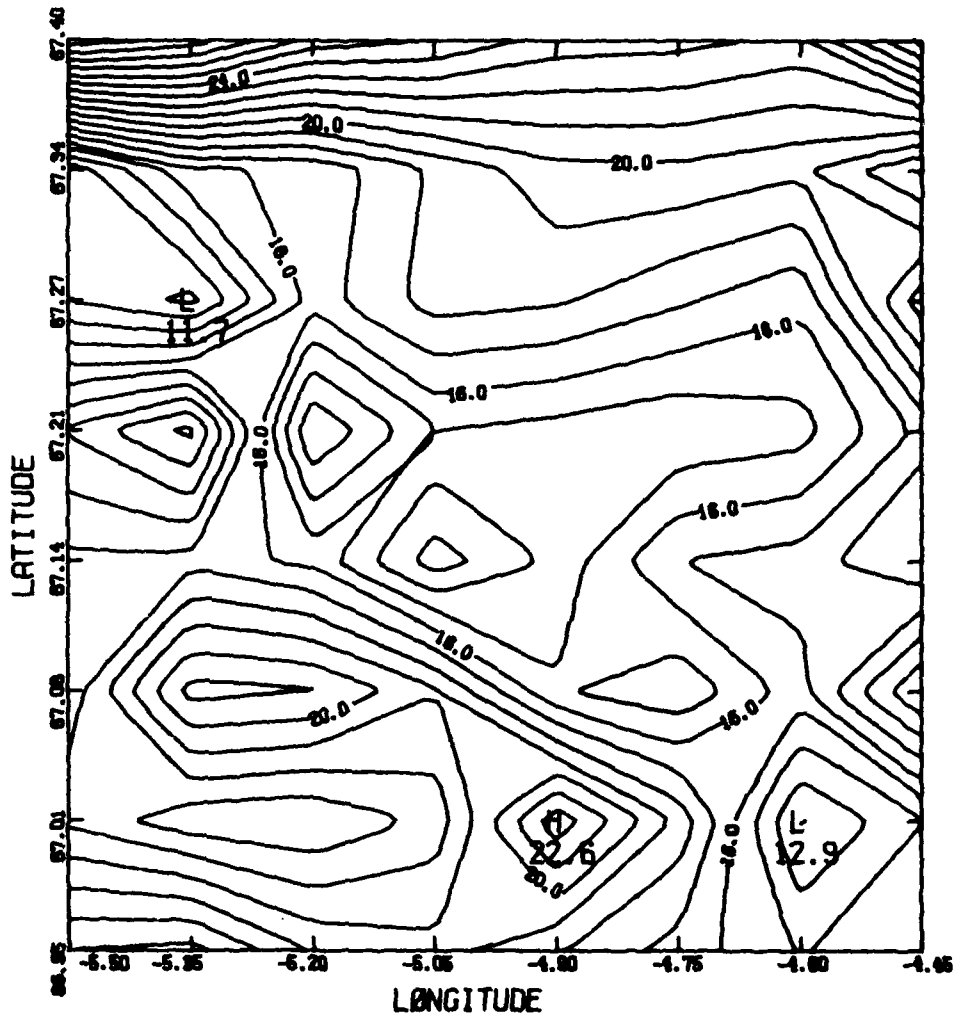


Figure 10 b)

OBJECTIVE MAPPING ERROR MAP

TEMPERATURE = 2°C

ERROR VARIANCE = 0.2000

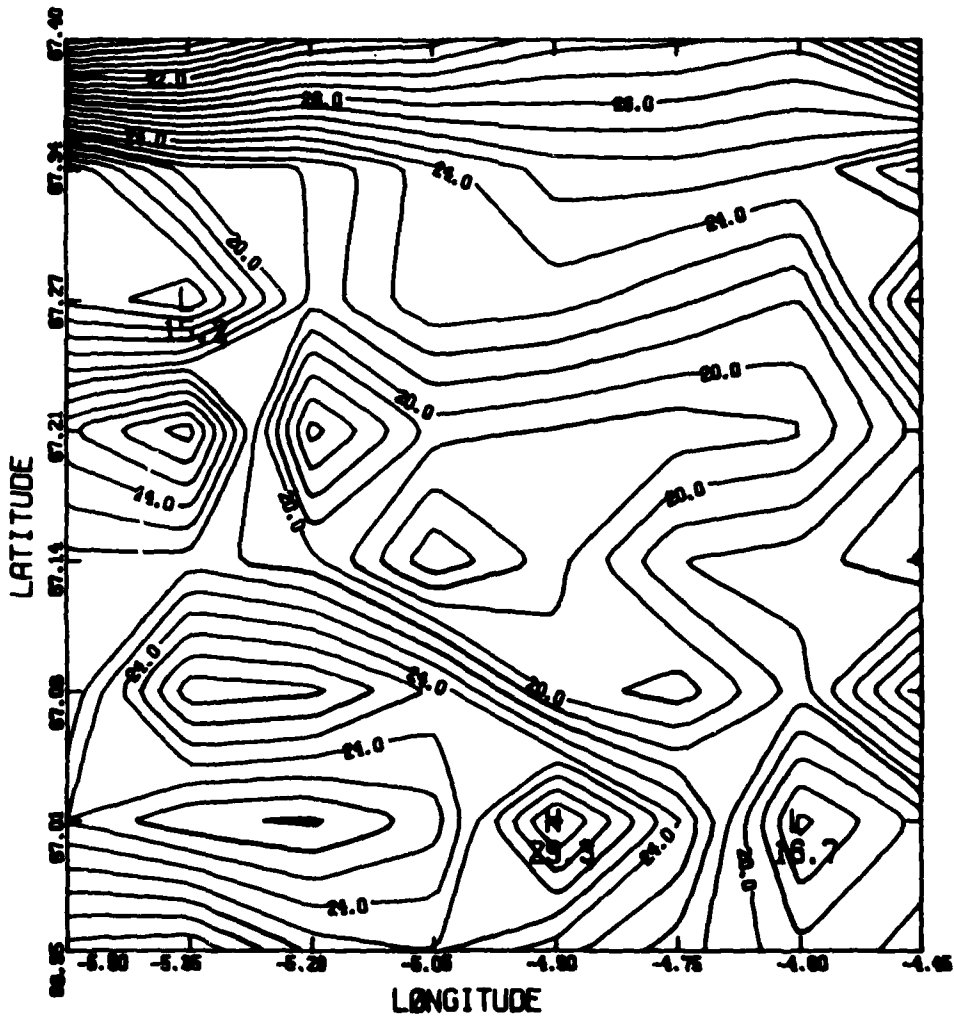


Figure 10 c)

OBJECTIVE MAPPING ERROR MAP

TEMPERATURE= 3°C

ERROR VARIANCE= 0.2000

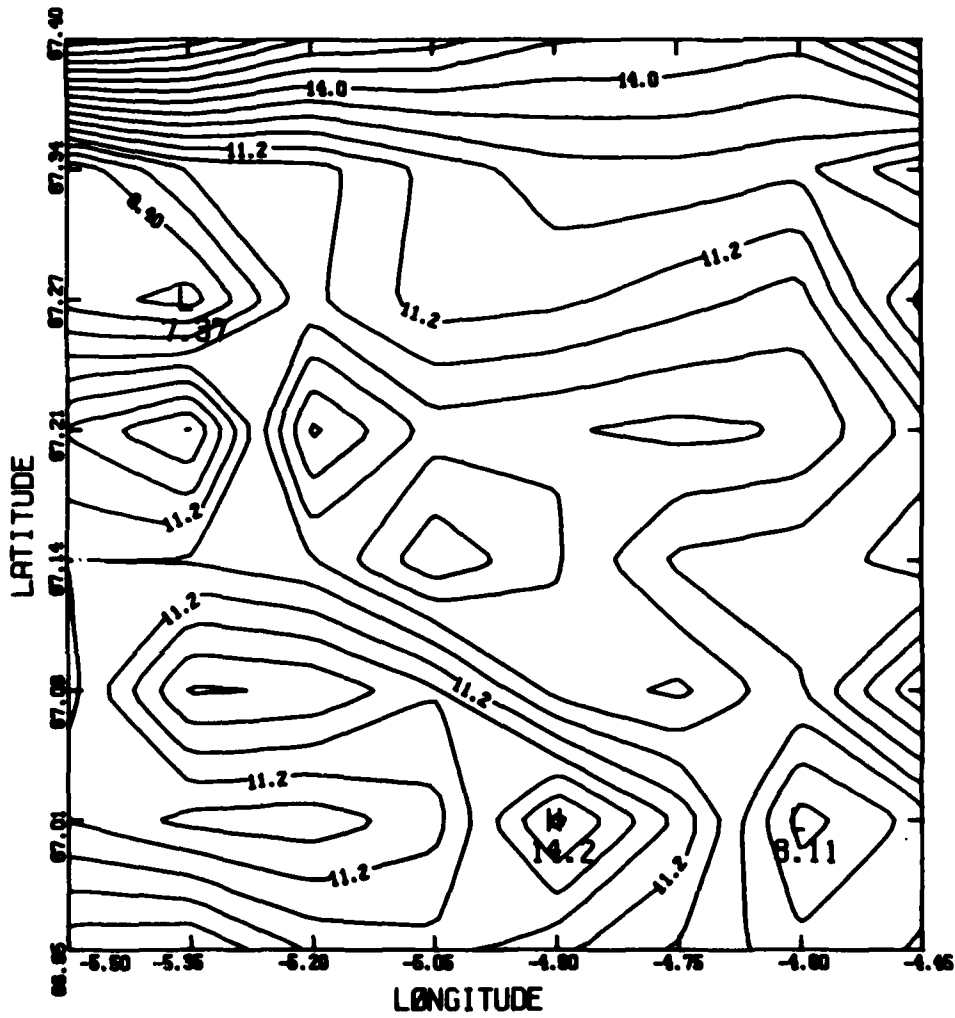


Figure 10 d)

Errors within an XBT cast, be they inferred depth or measured temperature, are most likely more correlated than errors between XBT casts. Consequently, the character of a single recorded profile will probably be at least qualitatively correct. An inferred isotherm surface based on observations from a number of XBTs with less-correlated errors, however, may not even be that. It will depend entirely on the nature of the isotherm surface vis-a-vis the magnitude of the XBT errors. In the segment of ocean we have analyzed in this report, we have deduced an rms isotherm depth fluctuation of only 40 m. What is the expected error in the inference of an isotherm depth from a single XBT drop? It is probably of comparable size.

As a result of the above deliberations, we would have to draw the following conclusions:

- 1) It is not possible to conduct a "frozen time" spatial survey of this size in this area with a single ship. The dynamics of the ocean modify the characteristics too quickly for spatial sampling. An aircraft survey using AXBTs would be more suitable--AXBT instrument problems notwithstanding.
- 2) Many more observations need be taken. The apparent smallness of spatial scales in this area requires a more dense set of data. Correlation between adjacent samples serves to improve statistical estimation. In the present data set there was practically no such correlation.
- 3) Because of potential problems in both the recorded temperature and the inferred depth, characterizing an area in terms of isotherm-depth surfaces using XBT data is probably not wise. The requirement of inferring the depth at which an absolute value of temperature occurs is too stringent for XBT measurements--especially when analysis depends on differences between XBT measurements. Mapping the depth of the main thermocline or mapping the thickness of the upper mixed layer might be amenable to XBT measurement. Neither depends on absolute temperature.

DISTRIBUTION LIST FOR TN 250

<u>Agency</u>	<u>Name/Code</u>	<u>No. of Copies</u>
Chief of Naval Operations Department of the Navy Washington, DC 20350	Dr. Edward Y. Harper OP-21T	1
Chief of Naval Operations Department of the Navy Washington, DC 20350	Dr. R. Clark OP-95T	1
Chief of Naval Operations Department of the Navy Washington, DC 20350	CDR H. L. Dantzler OP-952D3	2
Chief of Naval Operations Department of the Navy Washington, DC 20350	Mr. Art Bisson OP-21T3	2
Chief of Naval Research 800 North Quincy Street Arlington, VA 22217	Dr. R. W. Winokur Code 102C	2
Commanding Officer Naval Ocean Research and Development Activity NSTL, MS 39529	Dr. James E. Andrews Code 110	1
Commanding Officer Naval Ocean Research and Development Activity NSTL, MS 39529	Dr. S. A. Piacksek Code 322	1
Commanding Officer Naval Ocean Research and Development Activity NSTL, MS 39529	Dr. Albert Green Code 330	3
Commanding Officer Naval Ocean Research and Development Activity NSTL, MS 39529	Mr. C. R. Holland Code 252	1
Commanding Officer Naval Ocean Research and Development Activity NSTL, MS 39529	Dr. E. M. Stanley Code 340	1

DISTRIBUTION LIST FOR TN 250

<u>Agency</u>	<u>Name/Code</u>	<u>No. of Copies</u>
Commanding Officer Naval Ocean Research and Development Activity NSTL, MS 39529	Dr. Rudolph Hollman Code 340	6
Commanding Officer Naval Ocean Research and Development Activity NSTL, MS 39529	Mr. K. M. Ferer Code 340	1
Superintendent Naval Postgraduate School Monterey, CA 93940	Dr. Thomas R. Osborn Code 68 OR	1
Director Office of Naval Research 800 North Quincy Street Arlington, VA 22217	Dr. T. Spence Code 422PO	1
Director Office of Naval Research 800 North Quincy Street Arlington, VA 22217	Dr. E. A. Silva Code 420	1
Director Office of Naval Research Ocean Science and Technology Division ONR Detachment NSTL, MS 39529	LCDR Robert Willems Code 422PO	1
Commander Naval Ocean Systems Center San Diego, CA 92152	Dr. J. L. Losee	1
Commanding Officer U. S. Naval Oceanographic Office NSTL Station Bay St. Louis, MS 39520	Mr. W. S. Kamminga Code 7200	6
Commanding Officer Naval Research Laboratory 4555 Overlook Avenue, SW Washington, DC 20375	Dr. John P. Dugan Code 5810	6

DISTRIBUTION LIST FOR TN 250

<u>Agency</u>	<u>Name/Code</u>	<u>No. of Copies</u>
Defense Technical Information Center Building 5, Cameron Station Alexandria, VA 22314		12
Applied Physics Laboratory Johns Hopkins University Johns Hopkins Road Laurel, MD 20810	Dr. Gordon D. Smith	6
Aplied Physics Laboratory Johns Hopkins University Johns Hopkins Road Laurel, MD 20810	Dr. Larry J. Crawford	2
Applied Physics Laboratory Johns Hopkins University Johns Hopkins Road Laurel, MD 20810	Dr. Gordon E. Merritt	1
Applied Physics Laboratory Johns Hopkins University Johns Hopkins Road Laurel, MD 20810	Dr. Harold E. Gilreath	1
Applied Physics Laboratory Johns Hopkins University Johns Hopkins Road Laurel, MD 20810	Dr. D. Wendstrand	2
Applied Physics Laboratory University of Washington 1013 Northeast 40th Street Seattle, WA 98195	Dr. Michael C. Gregg	1
Applied Physics Laboratory University of Washington 1013 Northeast 40th Street Seattle, WA 98195	Dr. Thomas B. Sanford	1

DISTRIBUTION LIST FOR TN 250

<u>Agency</u>	<u>Name/Code</u>	<u>No. of Copies</u>
Applied Physics Laboratory University of Washington 1013 Northeast 40th Street Seattle, WA 98195	Dr. Eric D'Asaro	1
Johns Hopkins University Department of Chemical Engineering 34th and Charles Streets Baltimore, MD 21218	Mr. Michael Karweit	1
Marine Physical Laboratory Scripps Institution of Oceanography University of California, San Diego La Jolla, CA 92037	Dr. Rob Pinke1	2
Oregon State University School of Oceanography Corvallis, OR 97331	Dr. Rod Mesecar	1
University of South Florida Department of Marine Sciences 140 7th Avenue South St. Petersburg, FL 33701	Dr. A. D. Kirwan	2
Woods Hole Oceanographic Institution Woods Hole, MA 02543	Dr. Mel Briscoe	1
Marine Environments Corporation 10629 Crestwood Drive Manassa, VA 22100	Dr. Marshall D. Earle	1
Operations Research, Inc. 1400 Spring Street Silver Springs, MD 20910	Dr. Thomas Bell	2

DISTRIBUTION LIST FOR TN 250

<u>Agency</u>	<u>Name/Code</u>	<u>No. of Copies</u>
Science Applications, Inc. P. O. Box 1303 McLean, VA 22102	Dr. R. B. Lambert, Jr.	2
Sippican Corporation Ocean Systems Division P. O. Box 139 Marion, MA 02738	Mr. Richard W. Bixby	2
Commanding Officer U. S. Naval Oceanographic Office NSTL Station Bay St. Louis, MS 39529	Mr. J. Carroll Code 7000	1
Commanding Officer U. S. Naval Oceanographic Office NSTL Station Bay St. Louis, MS 39520	LCDR McMillan Code 3100	1
Commanding Officer U. S. Naval Oceanographic Office NSTL Station Bay St. Louis, MS 39520	R. Martine Code 3300	1
Commanding Officer U. S. Naval Oceanographic Office NSTL Station Bay St. Louis, MS 39520	L. Franc Code 3301	1
Commanding Officer U. S. Naval Oceanographic Office NSTL Station Bay St. Louis, MS 39520	W. Jobst Code 7300	3
Commanding Officer U. S. Naval Oceanographic Office NSTL Station Bay St. Louis, MS 39520	M. Shank Code 9000	3
Commander Naval Oceanography Command NSTL, MS 39529	CAPT Topaz	1

DISTRIBUTION LIST FOR TN 250

<u>Agency</u>	<u>Name/Code</u>	<u>No. of Copies</u>
Commander Naval Oceanography Command NSTL, MS 39529	CDR Miller	1
Commander Naval Oceanography Command NSTL, MS 39529	CDR Plante	1
Commanding Officer Naval Ocean Research and Development Activity NSTL, MS 39529	Mr. E. D. Chaika Code 270	2
Commanding Officer Naval Ocean Research and Development Activity NSTL, MS 39529	Mr. C. E. Stuart Code 260	3
Commanding Officer Naval Ocean Research and Development Activity NSTL, MS 39529	Mr. W. A. Kuperman Code 220	1
Commanding Officer Naval Ocean Research and Development Activity NSTL, MS 39529	R. B. Lauer Code 223	2
Commanding Officer Naval Ocean Research and Development Activity NSTL, MS 39529	J. H. Ford Code 240	1
Commanding Officer Naval Ocean Research and Development Activity NSTL, MS 39529	R. J. Van Wyckhouse Code 241	1
Commanding Officer Naval Ocean Research and Development Activity NSTL, MS 39529	Dr. R. A. Wagstaff Code 245	1

UNCLASSIFIED

SECURITY CLASSIFICATION OF THIS PAGE (When Data Entered)

REPORT DOCUMENTATION PAGE		READ INSTRUCTIONS BEFORE COMPLETING FORM
1. REPORT NUMBER NORDA Technical Note 250	2. GOVT ACCESSION NO.	3. RECIPIENT'S CATALOG NUMBER
4. TITLE (and Subtitle) Analyzing Temperature Data from XBT Grid Surveys	5. TYPE OF REPORT & PERIOD COVERED Final	
	6. PERFORMING ORG. REPORT NUMBER	
7. AUTHOR(s) Michael Karweit	8. CONTRACT OR GRANT NUMBER(s)	
9. PERFORMING ORGANIZATION NAME AND ADDRESS Naval Ocean Research and Development Activity Ocean Programs Management Office NSTL, Mississippi 39529	10. PROGRAM ELEMENT, PROJECT, TASK AREA & WORK UNIT NUMBERS	
11. CONTROLLING OFFICE NAME AND ADDRESS Same	12. REPORT DATE January 1984	
	13. NUMBER OF PAGES 44	
14. MONITORING AGENCY NAME & ADDRESS (if different from Controlling Office)	15. SECURITY CLASS. (of this report) UNCLASSIFIED	
	15a. DECLASSIFICATION/DOWNGRADING SCHEDULE	
16. DISTRIBUTION STATEMENT (of this Report) Approved for Public Release. Distribution Unlimited.		
17. DISTRIBUTION STATEMENT (of the abstract entered in Block 20, if different from Report)		
18. SUPPLEMENTARY NOTES		
19. KEY WORDS (Continue on reverse side if necessary and identify by block number) analysis of XBT data XBT measurements XBT errors grid survey spatial mapping objective analysis design of field experiments		
20. ABSTRACT (Continue on reverse side if necessary and identify by block number) This report considers a set of 78 XBT casts obtained by NAVOCEANO on the second leg of its cruise to the Norwegian Sea, spring 1981. The data were taken in a grid pattern over a rectangular segment of ocean 66.950-67.400N latitude and -5.600- -4.350W longitude, in a day and a half. The survey was to measure the spatial properties of the temperature field. This report analyzes the data with the perspective, and focuses on estimating isotherm surfaces as characterizations of the temperature field.		

DD FORM 1473
1 JAN 73

EDITION OF 1 NOV 65 IS OBSOLETE
S/N 0102-LF-014-6601

UNCLASSIFIED

SECURITY CLASSIFICATION OF THIS PAGE (When Data Entered)

END

DATE
FILMED

7 - 84

DTIC